https://doi.org/10.5194/essd-2025-833
Preprint. Discussion started: 15 January 2026

Open Access Earth System Science Data Discussions

A new, high-resolution global reef island database (GRID) with implications for coastal vulnerability

John L. Dawson

[1]College of Science and Engineering, James Cook University, Townsville, 4811, Australia

Correspondence to: John L. Dawson (john.dawson@my.jcu.edu.au)

Abstract. Low-lying reef islands (LRIs) are among the most climate-vulnerable landforms on Earth, yet no globally consistent and spatially comprehensive inventory of these islands has previously existed. This is especially important to underpin assessments of future risk and resilience. To address the absence of a unified global dataset, this study develops the first Global Reef Island Database (GRID), a detailed spatial product that identifies the global distribution of LRIs and collates their key geomorphological, environmental and exposure characteristics. Using the UNEP-WCMC Global Island Database (GID2.1), global coral reef distribution layers and the AW3D30 digital elevation model, all landmasses <30 km² located within 1 km of coral reef and below a conservative mean elevation threshold of 16 m were identified. A total of 34,404 LRIs were mapped accounting for nearly 11,000 km^2 of land area and over 60,000 km of shoreline. The vast majority (77%) are very small (<0.1 km^2) highlighting their geomorphological sensitivity. GRID demonstrates strong agreement with observed island counts (R^2 = 0.939; ICC = 0.984) and outperforms commonly used shoreline datasets in identifying small islands while preserving accurate geospatial alignment. LRIs are concentrated in Asia and Oceania, with Indonesia (14%), Japan (12%) and French Polynesia (10%) containing the largest numbers. For each island, eight intrinsic variables (including land area, elevation, shape, population and isolation) and ten extrinsic variables (including wave and tidal climate, bathymetry, tropical storm exposure and projected sea-level rise) were compiled to build a globally standardised dataset suited for vulnerability analysis. The GRID demonstrates clear spatial clustering in external forcing variables: wave exposure is highest across mid-ocean atolls, tropical storm density peaks in the northwest Pacific and Caribbean, and projected sea-level rise rates are greatest around the northern Philippines, Japan and Central America. Finally, this study develops an island vulnerability index using the GRID. Approximately 16% of LRIs are classified as very highly vulnerable, particularly throughout the northwest Pacific and northern South China Sea. National-scale assessments reveal that countries such as China, Japan and the Northern Mariana Islands are at highest risk. It is anticipated that thus far the most comprehensive yet unified database can support a variety of reef island research including climate adaptation planning, conservation and hazard mitigation efforts and coastal erosion studies. The final dataset has been made publicly available at https://doi.org/10.1594/PANGAEA.986811 (Dawson 2025).

https://doi.org/10.5194/essd-2025-833
Preprint. Discussion started: 15 January 2026

Open Access Earth System Science Data Discussions

1 Introduction

Islands associated with coral reefs have been occupied or used by humans for millennia (Nunn and Britton, 2001; Kayanne et al., 2011). The term reef island typically refers to "low islands" composed of unconsolidated biogenic carbonate sediments derived from reef biota as opposed to "high islands" composed of consolidated continental rocks (Fig. 1). Despite representing <1% of the total land area within the tropics, low-lying reef islands (LRIs) are extremely important geomorphological features, forming habitable and agricultural land that supports the livelihoods of hundreds of thousands of people, providing refuge for endemic and/or threatened species of flora and fauna, and supporting services essential to the economy of many island nations (Nunn et al., 2016; Kumar and Tehrany, 2017). LRIs are typically small (<0.5 km^2) low-lying accumulations of calcareous sediments derived from the detrital remains of organisms from the underlying reef (generally platform and atoll reefs). These sediments are transported by refracted waves and currents to a focal point on the reef flat where they are deposited. Over time, these deposits are able to build up above sea level, acquire a vegetation cover and become partially lithified. Maximum land elevation rarely exceeds 3-4 m and is often <2 m (e.g., Maldives, Tuvalu, Marshall Islands) (Perry et al., 2011; Nunn et al., 2020).

LRIs are widely considered one of the most vulnerable landforms on Earth to the impacts of global climate change (Perry et al., 2011; Nurse et al., 2014; Chand, 2020; Kumar et al., 2020). Climate-driven sea-level rise is arguably the single greatest threat to LRIs and the societies and ecosystems they support, and is expected to increase shoreline erosion, coastal inundation and saltwater intrusion into freshwater aquifers, reservoirs and agricultural crops (Nicholls and Cazenave, 2010; Becker et al., 2012; Albert et al., 2016; Karnauskas et al., 2016; Storlazzi et al., 2018; Falkland and White, 2020; Iese et al., 2020). Furthermore, increases in sea surface temperature, more frequent coral bleaching events and changes in ocean chemistry are expected to stress the calcifying reef organisms that supply sediment for island development and maintenance and/or provide a natural barrier to increasing wave energies (Perry et al., 2011; Hughes et al., 2017; Harris et al., 2018). Meanwhile, some LRIs have become so urbanized and densely populated (e.g., 47,400 people/km^2 on Male, Maldives and 8300 people/km^2 on Fongafale, Tuvalu) that local anthropogenic stresses (e.g., increased nutrients) are now a serious compounding issue (Osawa et al., 2010; Decarlo et al., 2015). These potential threats to future environmental and socioeconomic development of reef island nations call for a better understanding of dependent reef island vulnerabilities and provide the stimulus for this study.

There are various methods to assess coastal vulnerability including index-based methods (e.g, the Coastal Vulnerability Index), indicator-based approaches, GIS-based decision support tools and dynamic computer modelling (e.g., Delft3D). The index-based methods combine different parameters (physical and socio-economic) into a unitless index of vulnerability and are popular due to their relatively simple concept. The coastal vulnerability index (CVI), first developed by Gornitz and Kanciruk (1989) is the most widely used index and has been adopted worldwide in evaluating the risk to climate change, particularly sea-level rise (Gornitz et al., 1994; Thieler, 2000; Ahmed et al., 2022). A CVI would provide a simple numerical basis for ranking LRIs in terms of their potential risk to future climate change impacts. Given the perceived threats of future climate

https://doi.org/10.5194/essd-2025-833
Preprint. Discussion started: 15 January 2026

change to LRIs and the societies and ecosystems they support, it is ever-increasingly important to assess vulnerability using the best available globally comprehensive spatial data.

Numerous studies have investigated the distribution of islands at local and regional scales (Hopley et al., 2007; Webb and Kench, 2010; Kench, 2012; Sheppard et al., 2012; Ford, 2013; Nunn et al., 2016; Duvat et al., 2017b; Kumar and Tehrany, 2017; Nunn et al., 2020). However, the United Nations Environment Program (UNEP) Island Directory (Dahl, 1991) was a first step towards a global-scale overview, despite only providing information on ~2000 islands with little focus on LRIs. This data was improved upon and later summarised by Gillespie and Clague (2009) and a "Global Island Database" (GID) was made publicly available by the UN Environment Programme World Conservation Monitoring Centre (UNEP-WCMC) in 2010. Island geometries were based on the GSHHS (version 1) shoreline database of Wessel and Smith (1996) and included ~175,000 islands. UNEP-WCMC has since developed a second version of the GID with geometries based on Open Street Map® (OSM) data (Weatherdon et al., 2015), a global shoreline product which is freely available in the public domain (www.openstreetmap.org). The GID version 2.1 has geometric boundaries of over 400,000 islands ranging from 1 x 10^{-6} km^2 to 0.78 x 10^6 km^2 (Unep-Wcmc, 2015). More recently, the U.S. Geological Survey (USGS), in partnership with Esri, has developed Global Islands Explorer (GIE), a visualisation and query tool of global islands data based on the Global Vector Shoreline (GVS) derived from 30 m Landsat 7 data (Sayre et al., 2019) and includes over 340,000 islands of 0.036 km^2 and larger (https://rmgsc.cr.usgs.gov/gie/). Despite these recent improvements in spatial datasets of global shorelines, and the widespread perceptions of reef island vulnerability, there has surprisingly been limited focus on datasets of LRIs (Nunn et al., 2016; Nunn et al., 2020).

From a coastal management perspective, LRIs are inherently different from continental islands and mainland coastlines and exhibit a large variation in size, shape, elevation, geologic history, geographic isolation, and climatic conditions. Although the major process mechanism controlling formation and stability of LRIs is wave action and its interaction with the reef surface, several additional factors underpin the vulnerability of a particular island including island geomorphology, geographic isolation, regional sea level history, reef platform elevation and gradient, tidal regime, antecedent morphology and the availability of sand (Kench et al., 2009; Nunn et al., 2016; Nunn et al., 2020). However, standardised, globally-comprehensive inventories of reef island distribution, diversity and relative vulnerability are not yet available, but are important for regional planning on issues such as exposure to disasters, pollution and vulnerability to climate change, particularly sea-level rise. Furthermore, LRIs are often over-generalised in large-scale datasets when compared to continental islands and mainland coasts due to their relatively small land area, small human population size, and isolation (Nunn et al., 2016). To address these deficiencies, the main objective of this study is to present the first ever global spatial database of LRIs and their associated physical and environmental characteristics which can be used in local, regional or global studies that aim to assess coastal vulnerability to natural and/or anthropogenic impacts, and better inform regional and global management directives. The methods applied in this study utilise freely available global datasets in order to produce a global reef island database (GRID) and associated intrinsic and extrinsic characteristics that can be utilised within a CVI.

https://doi.org/10.5194/essd-2025-833
Preprint. Discussion started: 15 January 2026

2 Methods

2.1 Classification and mapping of LRIs

Historically, a distinction has been made between 'high' islands composed of continental rocks and 'low' islands composed of biogenic carbonate sediments produced by reef organisms (Stoddart and Steers, 1977; Hopley et al., 2007; Nunn et al., 2016) (Fig. 1). Hopley et al. (2007) and Nunn et al. (Nunn et al., 2016) provide detailed classifications of both types throughout the Great Barrier Reef and Pacific Ocean, respectively. For the purpose of this study, LRIs are defined as low-lying islands formed from sediments derived from the reef on which they sit and are often referred to as coral reef islands, coral cays, sand cays or motu. When developing the GRID, LRIs are defined as landmasses $\leq$30 km^2 located on or within 1 km of coral reef and with an elevation of $\leq$16 m (explained below). The size limit of 30 km^2 is somewhat arbitrary although it has been chosen based on the size of Diego Garcia, Chagos (29.7 km^2), one of the largest documented LRIs (Sheppard et al., 2012). Development of the GRID required the following workflow (Fig. 2) including: 1) the creation of a global shoreline vector file containing the geographic distribution of LRIs; and 2) the development of a comprehensive global database of LRIs including key geomorphological and environmental characteristics.

The GRID was initially derived from version 2.1 of the UNEP-WCMC Global Island Database, a global shoreline vector file based on geometry data from Open Street Map® (OSM) (Weatherdon et al., 2015). All post-processing was undertaken using industry standard GIS software (ArcGIS Pro®). The initial vector file was projected using the Mollweide projection, an equal-area pseudocylindrical map projection displaying the world as an ellipse with axes in a 2:1 ratio. Mollweide projection was chosen for its accurate derivation of area, especially in regions close to the equator, where most LRIs are located. The projected vector file contained a total of 465,558 island polygons of which 462,274 were less than 30 km^2 (excluding freshwater islands) and extracted for further analysis (Fig. 2).

The separation of LRIs from all other island types is based on two major criteria: 1) proximity to coral reef; and 2) elevation above mean sea level (MSL) (Fig.2). The coral reef layer that was used is the Global Distribution of Coral Reefs compiled by UNEP-WCMC, WorldFish Centre, WRI, TNC (2021). A select by location command was used to select and extract island polygons within a geodesic distance of 1 km from coral reef polygons. The mean elevation above MSL of each island polygon (in metres) was extracted from the ALOS Global Digital Surface Model (AW3D30 – downloaded on 30 June 2022 from https://www.eorc.jaxa.jp/ALOS/en/dataset/aw3d30/aw3d30_e.htm using the Zonal Statistics tool in ArcGIS Pro. The AW3D30 is a 1 arcsecond (~30 m at equator) resolution global digital elevation model (DEM) and considered one of the most accurate available (Caglar et al., 2018; Uuemaa et al., 2020). While the maximum elevation of most LRIs is typically less than ~4 m above MSL, a maximum mean elevation of 10 m above MSL has been chosen to account for LRIs that have developed aeolian or storm-generated ridges (Woodroffe, 2008; Hilton et al., 2019). An additional 6 m is included to account for vertical uncertainty in the AW3D30 DEM (Santillan et al., 2016). It should be noted that the AW3D30 model is a digital surface model which represents the elevation of tree canopy tops and building roofs, therefore mean elevation was found to be a more reliable classifier than maximum elevation. An assessment of derived elevations for several locations known to be exclusively

https://doi.org/10.5194/essd-2025-833
Preprint. Discussion started: 15 January 2026

composed of LRIs (e.g., Maldives, Marshall Islands and several atolls of the Tuamotu Archipelago) indicated that 16 m was a suitable threshold. Islands with a mean elevation of greater than 10 m (16 m including DEM uncertainty) above MSL are considered 'high islands' (volcanic, limestone, continental, composite) and are excluded from the dataset. Elevation data could not be retrieved for 408 islands (<2% of the database) although this was on most accounts due to very small island sizes in comparison to the 30 m cell size of the AW3D30 DEM. A further 739 islands were given negative mean and/or maximum elevations which could be due to very low elevations combined with a negative bias exhibited by the AW3D30 model (Caglar et al., 2018).

The attribute table (also supplied as a separate comma-separated text file – https://doi.org/10.1594/PANGAEA.986811) is sorted by IDs (*ID*) unique to each LRI. Latitude (*Lat*) and longitude (*Long*) were calculated for polygon mass centroids (Paris and Mitasova, 2014). Country/territory (*Country*) and sovereign (*Sovereign*) names as well as International Organization for Standardization (ISO 3166) country codes (*ISO3166*) were based on their respective economic exclusion zone (EEZ) using data from World EEZ v11 (www.marineregions.org) (Fig. 2). Island names were assigned using a combination of the NGA GEOnet Names Server (GNS) (downloaded on June 22, 2022, from https://geonames.nga.mil/gns/html/index.html) for all regions outside the United States, and the US Geological Survey Geographic Names Information System (GNIS) (downloaded on June 22, 2022 from https://www.usgs.gov/core-science-systems/ngp/board-on-geographic-names) for the United States and its overseas territories. Geographic names were filtered to only include those classified as singular islands. Supplementary names were also extracted from the global shoreline vector (GSV) (downloaded on June 20, 2022, from https://rmgsc.cr.usgs.gov/gie/). Geographic names from the GNIS, GNS and GSV were assigned to spatially intersecting island polygons in the GRID using a spatial join, and duplicated names for a given island were eliminated. Geographic coordinates derived from the GNS were relatively coarse for some regions resulting in a number of instances where GNS point locations did not intersect the island polygons in the GRID to which they correctly referred to. Therefore, a 300 m radius search was added to the intersect command during the spatial join to account for relatively small geographic disparities. This method considerably increased the number of LRIs in the GRID that were assigned a name, but at the expense of increasing the number of LRIs assigned the same name such as where distances between islands are very small (<300 m).

In total, 6084 LRIs were assigned single names, while in 6781 cases, more than one name was located inside an island polygon. This was either due to multiple names included in the GNS (e.g., various European and local/vernacular names are often assigned to a singular coordinate location), erroneously located names of closely adjacent LRIs, or on occasion, a limitation of the underlying OSM shoreline data (e.g., many small LRIs represented by one large island polygon in some large atolls of the Marshall Islands and French Polynesia). In these instances, all available names have been included in the GRID database (*IsName*) and the choice of a single representative name is left to the user. The attribution of island names is an ongoing process and far from completion. For example, 21,539 LRIs classified in the GRID are currently unnamed. However, it is anticipated that the majority of these probably represent small nameless sand cays and rocky outcrops. Future versions of GRID are planned to utilise data from the OSMNames project (https://osmnames.org/).

https://doi.org/10.5194/essd-2025-833
Preprint. Discussion started: 15 January 2026

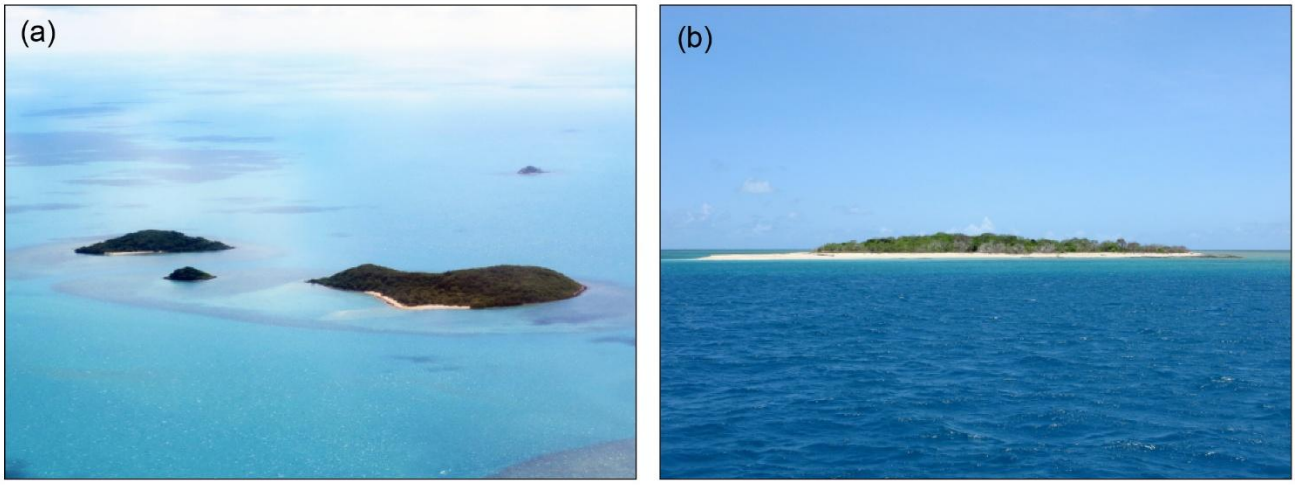

Figure 1: Reef Island types (a) 'High' islands composed of continental rocks and (b) 'Low' islands composed of biogenic material from the surrounding reef.

165

2.2 Intrinsic variables

Currently GRID contains eight intrinsic variables and ten extrinsic variables for each LRI. Human population estimates for each island polygon (*Popn*) are calculated by summing intersecting 3-arcsecond raster cells of constrained UN-adjusted population data for 2020 produced by WorldPop (downloaded on July 2, 2022 from https://www.worldpop.org/). WorldPop
170 is considered one of the most accurate gridded population distribution datasets currently available (Bai et al., 2018). To account for geographic discrepancies or where small LRIs did not fully encompass a population raster grid cell, a 200 m buffer was applied.

Island area (*Area*) and perimeter (*Length*) are calculated from each GRID polygon in a Mollweide equal-area projection and given in square kilometres and kilometres, respectively. Mean elevation (*Elev*) of each island was determined using AW3D30
175 global elevation data (see above). A dimensionless shape factor of $4\pi * Area/Length^2$ is used as a measure of island shape (*Circ*) with a value of one indicating a perfect circle. As a value approaches zero, it indicates an increasingly elongated and complex shape. Shape has an important influence on sensitivity and physical resilience of LRIs to changing boundary conditions. For example, circular LRIs are typically considered less susceptible to long-term coastal erosion than more irregular shaped LRIs because of their greater capacity for landform adjustment (Kench and Brander, 2006; Kumar et al., 2018; Sengupta et al.,
180 2025).

Contemporary LRIs are geologically young having predominantly developed over the last 3-4 thousand years (Kench et al., 2014; East et al., 2018). The reef type (*Reef*) was classified as either Atoll or Barrier/fringing according to the global

https://doi.org/10.5194/essd-2025-833
Preprint. Discussion started: 15 January 2026

Open Access Earth System Science Data Discussions

distribution of coral reefs dataset compiled by UNEP World Conservation Monitoring Centre (UNEP-WCMC) and supplemented by data collected by ReefBase (http://www.reefbase.org/main.aspx).

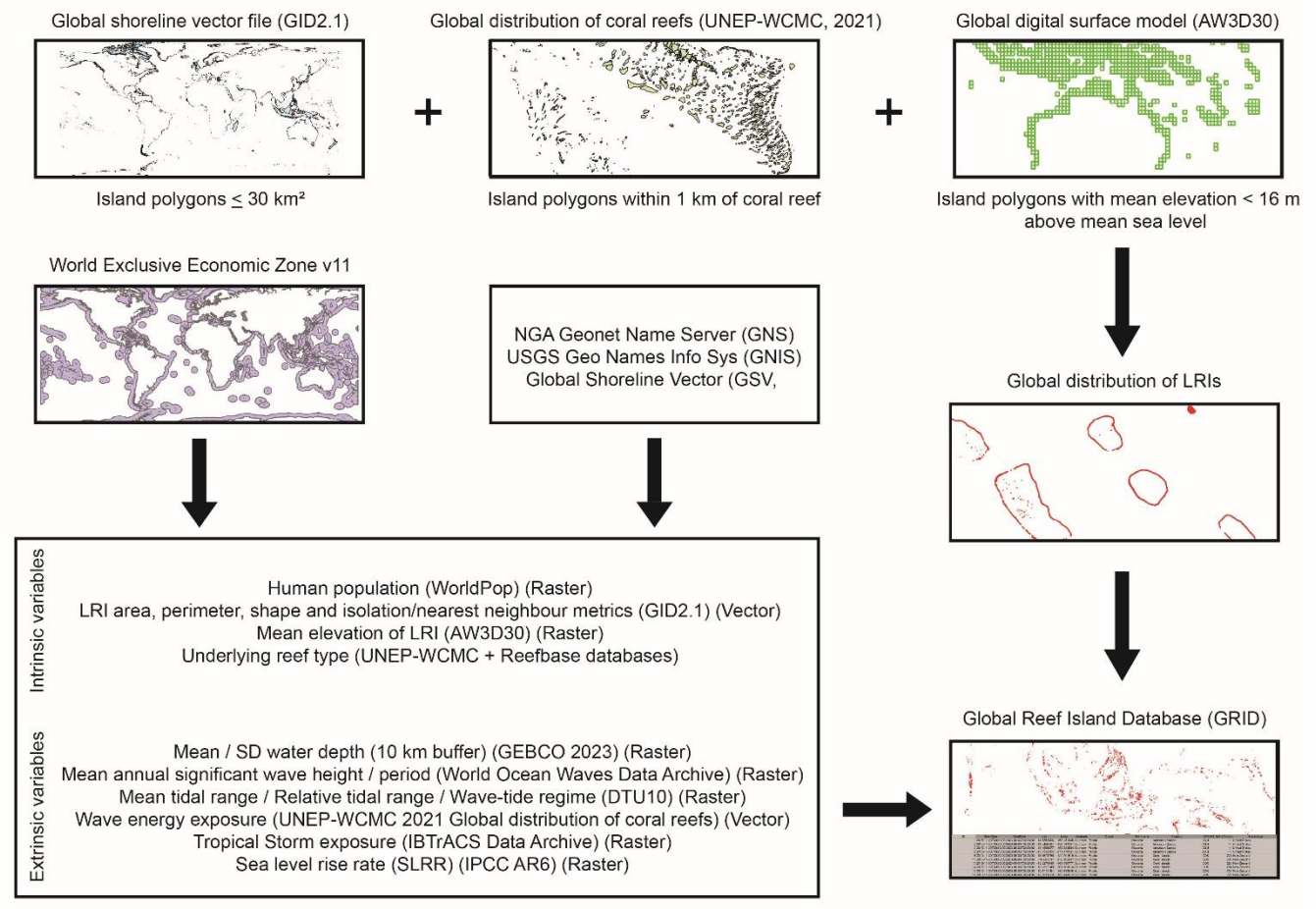

Figure 2: Work flow followed for the development of the Global Reef Island Database (GRID).

Geographic isolation (*Isol*) is calculated as the sum of the proportions of land area (including continental mainland) within buffer distances of 100, 1000, and 10,000 km around each island's perimeter (Diver 2008; Weigelt and Kreft, 2013; Weigelt et al., 2013) and normalised on a scale of zero to one with values closer to zero surrounded by a greater percentage of land (least isolated) and values closer to one surrounded by lowest proportions of land (most isolated). Unlike other measures of isolation, such as distance to nearest mainland, the proportion of surrounding landmass accounts for coastline shape and more accurately reflects true isolation, especially in congested island archipelagos (Diver, 2008). The distance between each LRI and its closest neighbouring LRI (*Near*) was also included as a measure of inter-island isolation (Diver, 2008).

https://doi.org/10.5194/essd-2025-833
Preprint. Discussion started: 15 January 2026

2.3 Extrinsic variables

The mean water depth (*Depth*) and associated standard deviation (*DepthSD*) surrounding each LRI was extracted from the General Bathymetric Chart of the Oceans (GEBCO 2023) (downloaded on August 3, 2023, from https://www.gebco.net) using a 10 km buffer. Surrounding bathymetry can be useful in distinguishing oceanic atoll islands from continental platform/barrier reef islands and as a proxy for relative exposure to wave energy.

Mean annual significant wave height (*MAWH*) and mean annual wave period (*MAWP*) for each island was taken from a 2-degree global grid of monthly means between 1888-2015 (World Ocean Waves Data Archive, http://www.sail.msk.ru/wow/). Where island polygons overlaid grid cells with no data (mostly those close to major coastlines or throughout the Indonesian archipelago) a focal mean of the surrounding grid cells was calculated. The mean tidal range (*MTR*) for each LRI was calculated using the DTU10 global ocean tide model (https://www.space.dtu.dk) at a resolution of 0.125-degree cell size.

The morphology of LRIs is not simply dependent on absolute wave height or tidal range, but on the interaction between the two (Kench and Brander, 2006). This can be represented by the relative tidal range (*RTR*) which is given as the ratio of tidal range to mean annual wave height (*MTR*/*MAWH*) (Davis and Hayes, 1984, Masselink and Short, 1993, Stutz and Pilkey, 2011). Large values of *RTR* indicate tidal dominance while small values signify wave dominance. The wave-tide regime (*WTReg*) for each LRI was then classified using the relationships suggested by Davis and Hayes (1984) and used by Stutz and Pilkey (2011) to classify barrier islands.

Coral reefs are highly efficient natural barriers surrounding LRIs. Wave energy diminishes with increasing reef width (Sheppard et al., 2005; Kench and Brander, 2006; Ferrario et al., 2014) therefore LRIs surrounded by a larger proportion of reef would be expected to have a relatively higher level of protection against high energy events such as storm surges. Therefore, the proportion of coral reef within a 10 km buffer distance of each island polygon perimeter is used as a measure of relative wave exposure (*WExp*): LRIs with a greater proportion of surrounding reef being less exposed to wave action.

A relative tropical storm exposure (*TSExp*) is calculated for each LRI based on a global 0.1° raster grid of storm density. In this study, storm density is defined as the number of tropical storms (Saffir-Simpson Hurricane Scale $\geq$ -1) per year within a 200 km search radius using the IBTrACS dataset (1851-2022, downloaded from https://www.ncdc.noaa.gov/ibtracs/ on 02/02/2022).

Finally, a year-2100 projected median sea level rise rate in mm yr^{-1} (*SLRR*) is assigned to each LRI in the GRID using a global 1° raster grid created from the latest iteration of the IPCC (AR6) projections using the medium-high reference Shared Socio-economic Pathway (SSP) 3-7.0 dataset stored on the PO.DAAC Drive (https://podaac-tools.jpl.nasa.gov/drive/files/misc/web/misc/IPCC) – see Meinshausen et al. (2020) for descriptions of SSPs.

https://doi.org/10.5194/essd-2025-833
Preprint. Discussion started: 15 January 2026

Open Access Earth System Science Data Discussions

3 Results

A total of 34,404 individual LRIs are contained within GRID and are distributed throughout tropical regions of the world's oceans (Fig. 3a). Globally, LRIs amass to a total land area of 10,899 km^2 (0.007% of world's total and 0.022 % of land contained within the tropics) and 60,742 km of shoreline. The continents of Asia and Oceania account for 42% and 32% of the total number, 43% and 34% of the total land area, and 40% and 36% of the total length of coastline, respectively (Table 1). Approximately 80% of the world's LRIs occur in the top 20 countries/territories by number (Fig,3b, Table S1). Of the world's total, 14% of LRIs (4,762) occur in Indonesia, 12% (4,203) belong to Japan and 10% (3,308) are found throughout French Polynesia. LRIs belonging to Indonesia and Japan predominantly (> 99%) occur on barrier or fringing reefs while about 94% of LRIs throughout French Polynesia occur on atoll reefs.

The total population of people living on LRIs is estimated to be approximately 2.6 million, although only a very small proportion of LRIs are inhabited (~14%). Human occupation of LRIs is highest in the Philippines (~499,000), the Maldives (~494,000) and Indonesia (~419,000) (Figs. 3c, 4a) as well as the United States of America (USA) (~260,000) and the United Arab Emirates (UAE) (~104,000).

Island sizes show a strongly right-skewed distribution with 32,483 LRIs (94% of the total dataset) smaller than 1 km^2 and 26,596 LRIs (77%) smaller than 0.1 km^2 (Fig. S1). The global average size of LRIs is 0.3 km^2 while the largest LRI in the dataset is Diego Garcia, British Indian Ocean Territory at 30 km^2. The global average length of shoreline (perimeter) of LRIs is 1.8 km, while some mid-ocean atoll LRIs can have over 100 km of shoreline. The size and shape of LRI's is attributed to several factors, including reef morphology, accommodation space, availability of sediment and the prevailing hydrodynamic regime. Morphological characteristics of LRIs such as size and length show high spatial variability globally and are randomly distributed throughout the world's oceans (Figs. 4b, 4c, Moran's $I = 0.012$ and 0.024, respectively). However, mean elevation and shape (circularity) display a slight positive spatial dependence in comparison (Figs. 4d, 4e, Moran's $I = 0.095$), although still relatively weak.

Table 2 summarises island distribution according to latitude, reef setting and wave-tide regime. Of the total, 59% of LRIs occur in the northern hemisphere and 41% in the southern hemisphere. Approximately three quarters of all LRIs have developed upon barrier reefs or fringing reefs while the remaining quarter are found on Atoll reefs. LRIs of atoll origin are primarily located throughout the central and western Pacific as well as throughout the mid-Indian Ocean atoll chains of the Maldives and Chagos (Fig. 4f). The size of LRIs as well as their length of shoreline are significantly greater for atoll reefs in comparison to barrier/fringing reefs (Mann-Whitney, $p < 0.01$).

https://doi.org/10.5194/essd-2025-833
Preprint. Discussion started: 15 January 2026

Open Access Earth System Science Data Discussions

Table 1. Geopolitical distribution of LRIs derived from GRID showing total number of islands, total land area and total length of coastline. Percentages are of the world's total.

Continent	Islands (n)	(%)	Area (km^2)	(%)	Length (km)	(%)
ASIA	14,580	42	4,663	43	22,109	36
South China Sea/Indonesia	5,992	17	2,855	26	12,298	20
Pacific Ocean	5,308	15	368	3	2,250	4
Indian Ocean	2,232	6	838	8	4,735	8
Red Sea	779	2	403	4	1,947	3
Persian Gulf	269	1	199	2	880	1
OCEANIA	10,985	32	3,699	34	24,251	40
Pacific Ocean	9,747	28	3,068	28	21,495	35
Great Barrier Reef	782	2	160	1	1,176	2
Indian Ocean	456	1	472	4	1,580	3
AFRICA	2,494	7	1,181	11	5,578	9
Indian Ocean	2,036	6	743	7	3,940	6
Red Sea	458	1	438	4	1,638	3
NORTH AMERICA	5,844	17	1,257	12	8,021	13
Caribbean Sea	4,884	14	1,154	11	7,097	12
Pacific Ocean	751	2	52	<1	477	1
Gulf of Mexico	121	<1	37	<1	336	1
Atlantic Ocean	88	<1	14	<1	111	<1
SOUTH AMERICA	501	1	98	1	783	1
Caribbean Sea	324	1	81	1	605	1
Atlantic Ocean	129	<1	14	<1	136	<1
Pacific Ocean	48	<1	3	<1	42	<1
WORLD TOTAL	34,404		10,899		60,742	

https://doi.org/10.5194/essd-2025-833
Preprint. Discussion started: 15 January 2026

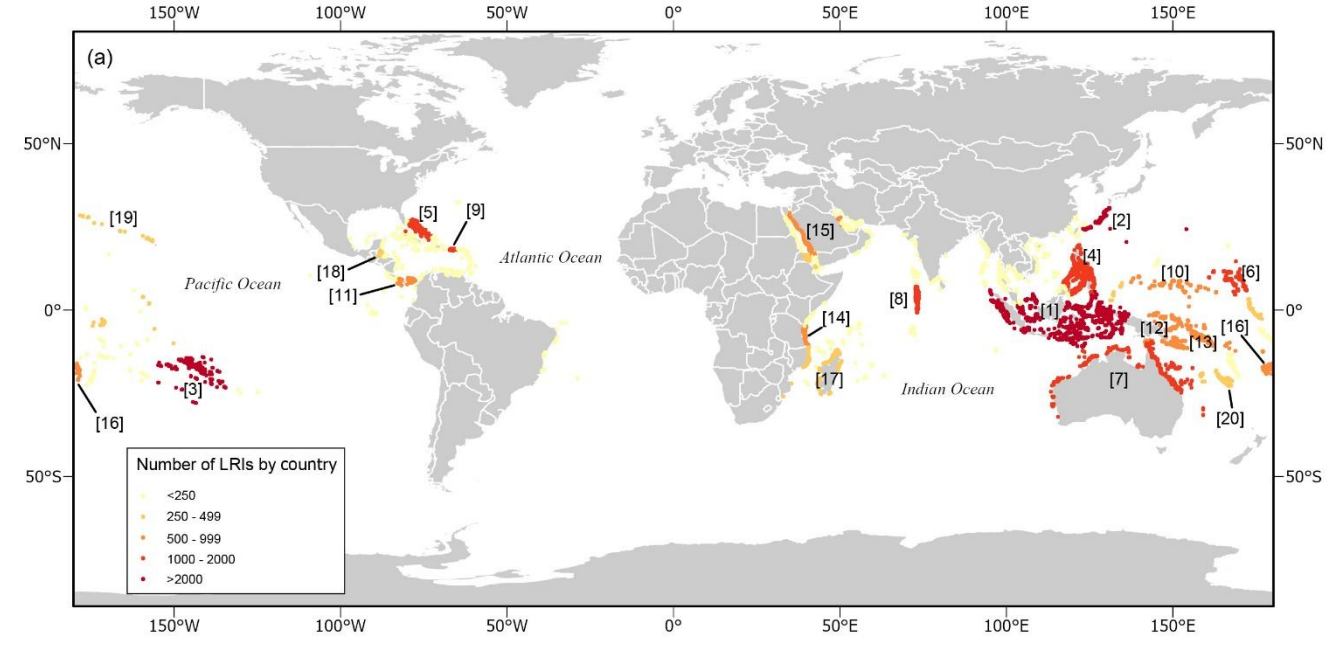

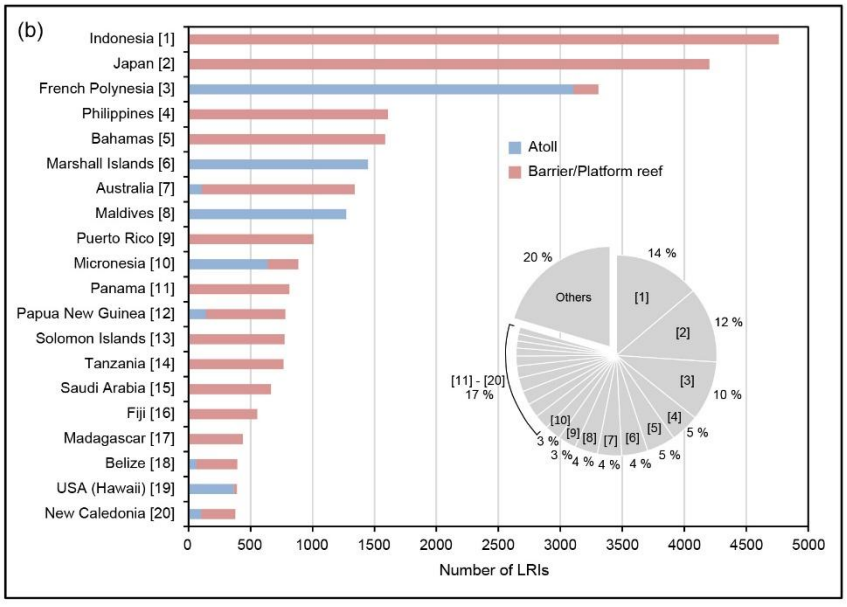

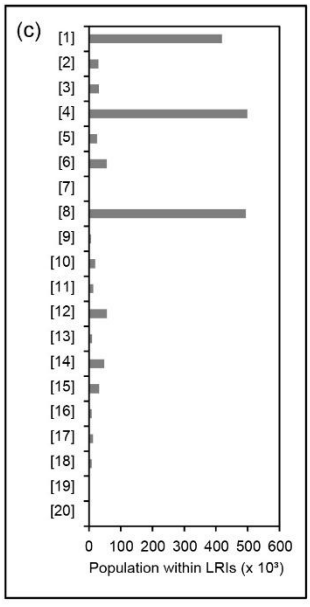

265

Figure 3: Top 20 countries based on total number of LRIs: (a) global spatial distribution, (b) total number of LRIs and the underlying reef type, and (c) human population estimates.

https://doi.org/10.5194/essd-2025-833
Preprint. Discussion started: 15 January 2026

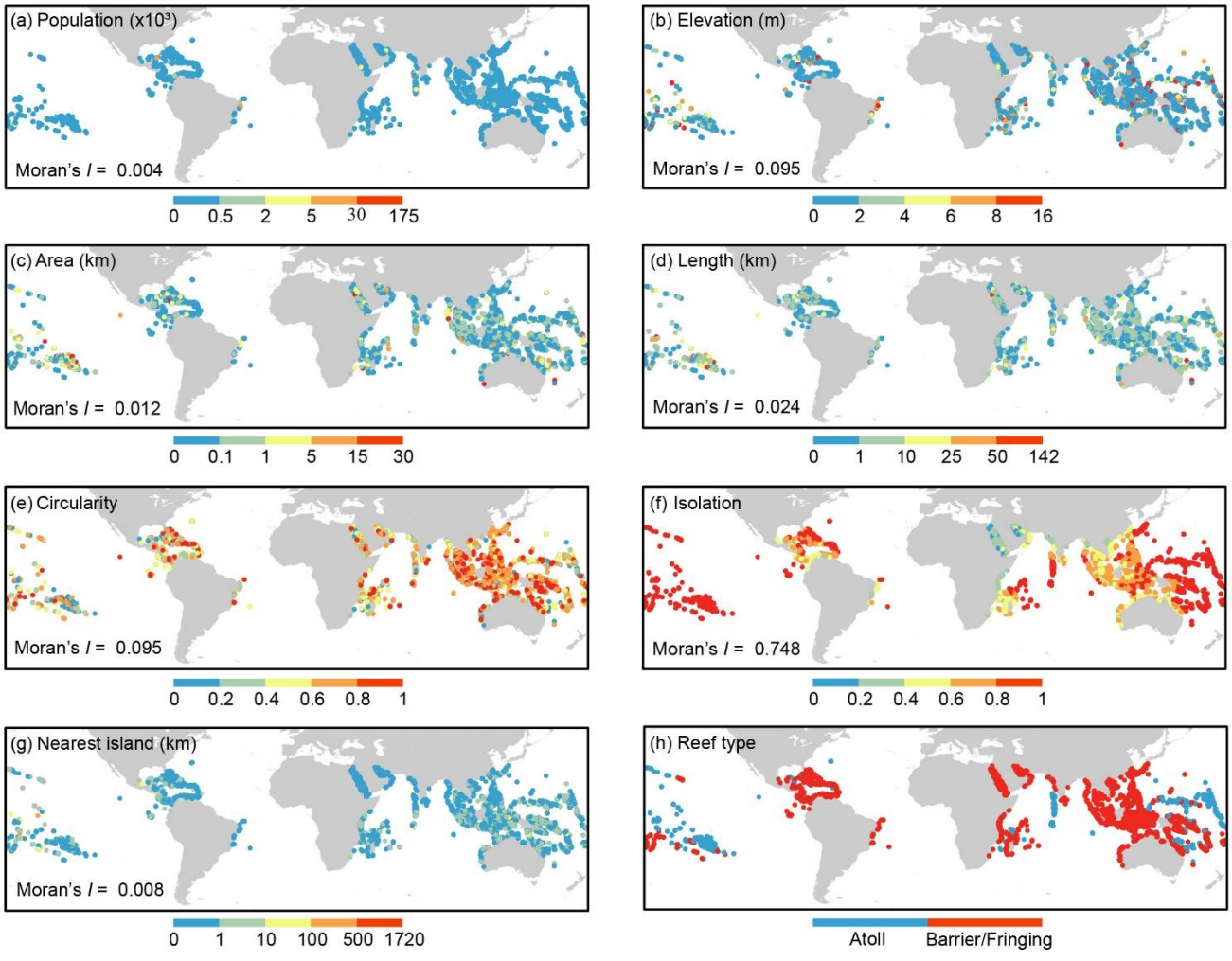

Figure 4: Global distribution maps for intrinsic variables (a-h) of LRIs included within GRID.

Island isolation is an important driver of species richness and is measured in this study using the proportion of surrounding landmass (Weigelt et al., 2013; Weigelt and Kreft, 2013). The most isolated LRIs are primarily located throughout the central and western Pacific Ocean, the East China Sea, central and western Indian Ocean and the northern Caribbean (Fig. 4g). Conversely, the least isolated LRIs are mostly located throughout the Red Sea, the Persian Gulf, the east coast of Africa and coastal regions of India and China. Intra-island isolation (distance to the nearest island) is spatially homogeneous and randomly distributed throughout the world's LRIs (Fig. 4h, Moran's $I = 0.008$).

https://doi.org/10.5194/essd-2025-833
Preprint. Discussion started: 15 January 2026

Open Access Earth System Science Data Discussions

Table 2. Distribution of LRIs by latitude, reef setting and wave-tide regime derived from GRID.

Geographic setting	Islands (n)	(%)	Area (km^2)	(%)	Length (km)	(%)
HEMISPHERE						
Northern	20,207	59	5,612	51	30,856	51
Southern	14,197	41	5,287	49	29,887	49
REEF SETTING						
Barrier/Fringing	26,105	76	8,216	75	41,390	68
Atoll	8,299	24	2,683	25	19,352	32
WAVE-TIDE REGIME						
Wave-dominated	15,949	46	4,813	44	30,455	50
Mixed Wave-dominated	11,416	33	2,904	27	16,491	27
Mixed tide-dominated	5,815	17	2,583	24	11,379	19
Tide-dominated	1,224	4	599	5	2,417	4

LRIs are generally highly spatially clustered throughout the GRID with respect to extrinsic variables (Fig. 5). Unsurprisingly, most LRIs located throughout the mid-ocean atolls of the Pacific have the deepest surrounding bathymetry and greatest exposure to large swell waves (Figs. 5a-5d). Mean tidal range and relative tidal range are generally greater for LRIs in the northern hemisphere compared to the southern hemisphere (Figs. 5e, 5f). Of the islands, 80% are wave dominated, 18% are mixed energy (wave or tide dominated) and less than 2% are tide dominated (Fig. 5g, Table 2).

LRIs surrounded by a larger proportion of reef would be expected to have a relatively higher level of protection (lower exposure) against high energy waves (Ferrario et al., 2014; Beetham et al., 2017). Relative wave exposure displays high spatial variability globally (Fig. 5h, Moran's $I = 0.111$). Countries/territories with the greatest proportion of surrounding reef (lowest relative wave exposure) include Bermuda, the Cocos Islands, Sudan/Egypt, Johnston Atoll, and the Glorioso Islands. LRIs that have developed on atoll reefs have a ~30% lower mean relative wave exposure than those that have formed on barrier or fringing reefs.

LRIs are significantly spatially clustered with respect to tropical storm exposure (Moran's $I = 0.835$, $p < 0.01$) with greatest exposure exhibited throughout the Caribbean and the northwest Pacific (Fig. 5i), especially throughout the Paracel Islands and Japan with a mean ± SD tropical storm density (number of storms per year within 200 km) of 0.520 ± 0.036 and 0.518 ± 0.058, respectively. For comparison, the 1,272 LRIs throughout the Maldives have a mean ± SD storm density of just 0.005 ± 0.003.

https://doi.org/10.5194/essd-2025-833
Preprint. Discussion started: 15 January 2026

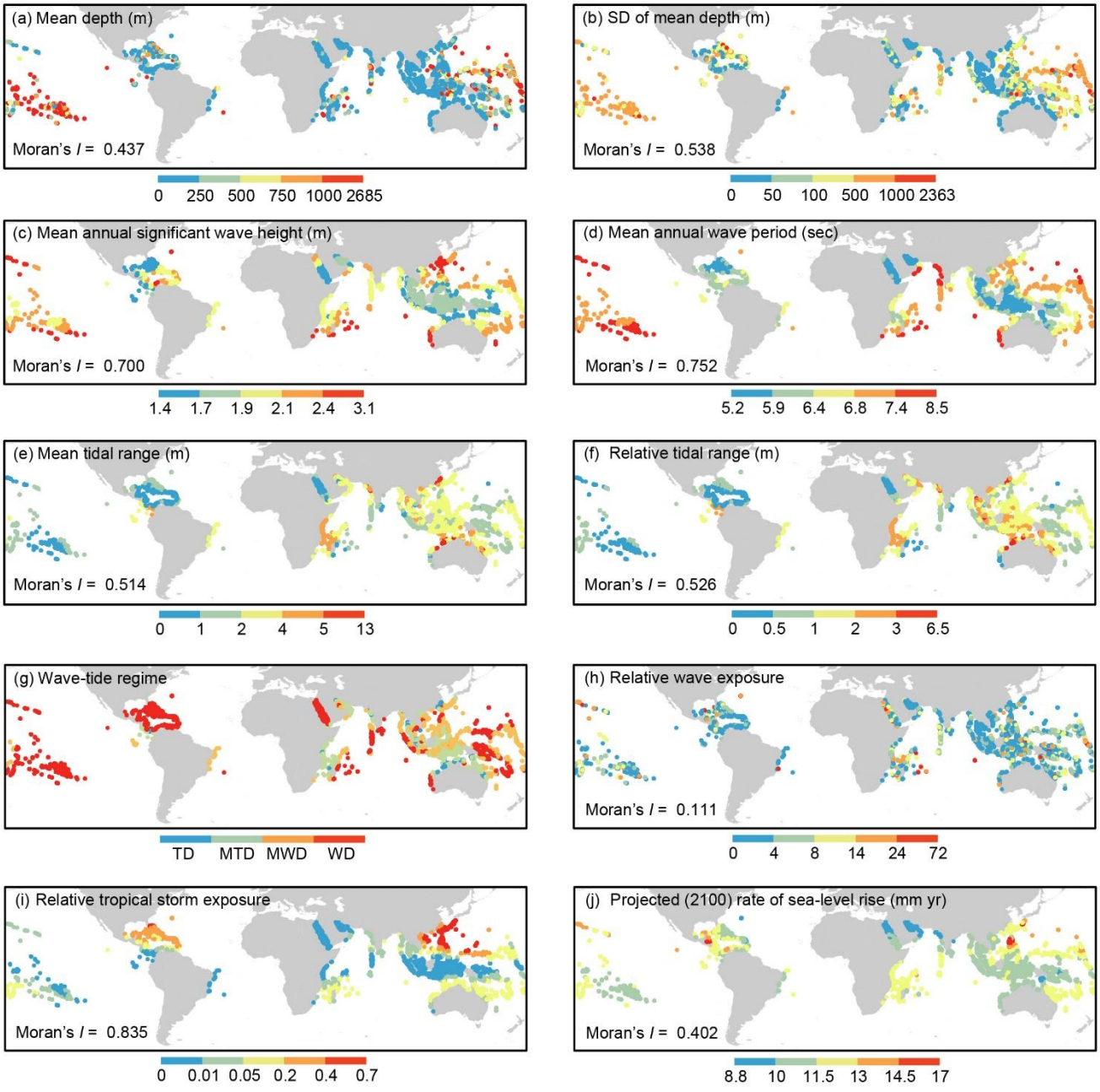

Figure 5: Global distribution maps for extrinsic variables (a-j) of LRIs included within GRID.

Finally, LRIs contained within GRID are shown to exhibit year-2100 projected median rates of sea-level rise of between 8.8 mm yr^{-1} (far northern Great Barrier Reef) and 15.1 mm yr^{-1} (northern Philippines). LRIs are spatially clustered with respect to future sea-level rise (Moran's $I = 0.402$, $p < 0.01$). Projected rates are lowest for LRIs within the Persian Gulf, the northern

https://doi.org/10.5194/essd-2025-833
Preprint. Discussion started: 15 January 2026

Red Sea and between Australia and Papua New Guinea and highest for LRIs off the coast of central America, the northern Philippines and south of Japan (Fig. 5j). Median projected rates for LRIs by country are greatest for Belize and Honduras (median: 14.6 mm yr^{-1}) and lowest for Kuwait (9.2 mm yr^{-1}).

4 Validation/quality assessment

4.1 Validation using published data

A set of published studies containing data on the number of LRIs occurring in twelve reef locations throughout the Atlantic, Indian and Pacific oceans was assessed and compared to numbers derived from the GRID (Table 3). Numbers of LRIs contained in the GRID are notably consistent with those quoted in the literature. A regression analysis performed over all of the available studies (n =12) resulted in an R^2 value of 0.96 with a slope of 1.06x indicating that the GRID slightly overestimates the number of LRIs compared to real-world observations (Fig. S2). However, the sample size is small and there is no way to assess the consistency between methods used in the studies to determine the number of LRIs. Furthermore, it is important to note that LRIs are dynamic landforms and may appear, split, merge, or disappear over short timescales. For example, in 2012 there were seven documented LRIs in the Dry Tortugas, Florida Keys (Bentley and Nittrouer, 2012). However, the reef has historically supported at least eleven LRIs, of which six disappeared between 1775 and 1975 due to high energy storm events such as hurricanes (Stoddart and Fosberg, 1981).

Table 3. A comparison between number of LRIs in GRID and numbers quoted in published studies.

Region	GRID	Published values	Source
Belize Barrier Reef	402	450	Murray et al. (1999)
Chagos	63	55	Dunne et al. (2012)
Cocos Keeling Islands	22	27	Lavers et al. (2019)
Cook Islands (Aitutaki and Manuae)	29	15	Summerhayes (1971)
Dry Tortugas, Florida Keys	6	7	Bentley and Nittrouer (2012)
Great Barrier Reef and Torres Strait	789	1000	Hopley et al. (2007)
Houtman Abrolhos	99	122	Evans et al. (2022)
Kwajalein Atoll, Marshall Islands	130	97	Dvorak (2018)
Maldives	1272	1190	Khan et al. (2002)
Marshall Islands	1448	1225	Baker et al. (2011)
Raroia, Tuamotus	121	280	McLean (2011)
Tuvalu	58	113	McLean (2011)

https://doi.org/10.5194/essd-2025-833
Preprint. Discussion started: 15 January 2026

4.2 Validation using global satellite imagery

A total of 200 reefs were randomly selected from the world's oceans according to a criterion of having at least one LRI present. This was undertaken by selecting LRIs from the GRID using the Subset Features tool in ArcGIS Pro® and counting the number of LRIs that occur on the underlying reef determined using ESRI's World Image Basemap. Zoom level was typically held at 1:5000 for counting purposes. In 13 instances, more than one LRI were randomly selected on a given reef. Therefore, additional reefs were randomly selected until the validation dataset included 200 separate reefs. The final validation dataset consisted of 141 barrier/finging reefs and 59 atolls reefs with a total of 4,130 observed LRIs (Fig. S3).

For a quantitative evaluation of the accuracy of the GRID-determined distribution of LRIs against locally observed (satellite-determined) ones, various statistical parameters were calculated including the coefficient of determination R^2, the root mean square error (RMSE), the mean bias error (MBE) and the intra-class correlation coefficient (ICC). The ICC is derived from a two-way random effects, absolute agreement, multiple measurements model (ICC2k) (Koo and Li, 2016). The ICC is included as a measure of agreement that accounts for both correlation and systematic bias in measurements that reduce reliability (Kirtman et al., 2013). All statistical analyses were conducted using XLSTAT®.

It should be noted that there is a high probability of temporal differences between predicted and observed data because: 1) both the GID2.1 shoreline vector file behind the GRID and ESRI's World Image used for validation are merged products from temporally varying datasets; and 2) LRIs are dynamic landforms and can develop or disappear in short periods of time in response to external drivers such as tropical storms (Maragos et al., 1973; Duvat et al., 2017a; Hoeke et al., 2021). Therefore, it is expected that part of the calculated errors is due to potential temporal incoherence.

A regression analysis performed over all validation data (n = 200) resulted in an R^2 value of 0.784. However, a significant outlier was discovered in the dataset that was distorting the analysis. A visual assessment confirmed that the outlier was an atoll reef (Midway Atoll) and that the creation of the shoreline dataset used for GRID had falsely identified breaking waves on the reef periphery as 303 LRIs. Therefore, removal of the outlier was justified. Only one such case was found in the validation dataset. Reperforming the regression analysis after outlier removal (n = 199) resulted in an R^2 value of 0.939 (p < 0.01) and an RMSE of 12.276 (Fig. 6a) indicating that LRIs derived from GRID captured the spatial variability ground truth data (satellite image-derived LRIs). The 95% confidence intervals of the model indicate that the true number of LRIs globally is most likely between ~32,000-35,000. There is almost negligible bias when comparing predicted (GRID) and observed (satellite) data (MBE = 0.181) indicating that the regression model only slightly under-predicts measured data (Fig. 6b). A reliability analysis resulted in an ICC2k value of 0.984 (CI: 0.979-0.988, p < 0.01) demonstrating excellent reliability (agreement) between predicted (GRID) and observed (satellite) data. Furthermore, according to the approach of Bland and Altman (1990), it is unlikely (<0.05 probability) that measurement pairs (predicted vs observed) of LRIs for a given reef would differ by more than 24 (Fig. 6b).

https://doi.org/10.5194/essd-2025-833
Preprint. Discussion started: 15 January 2026

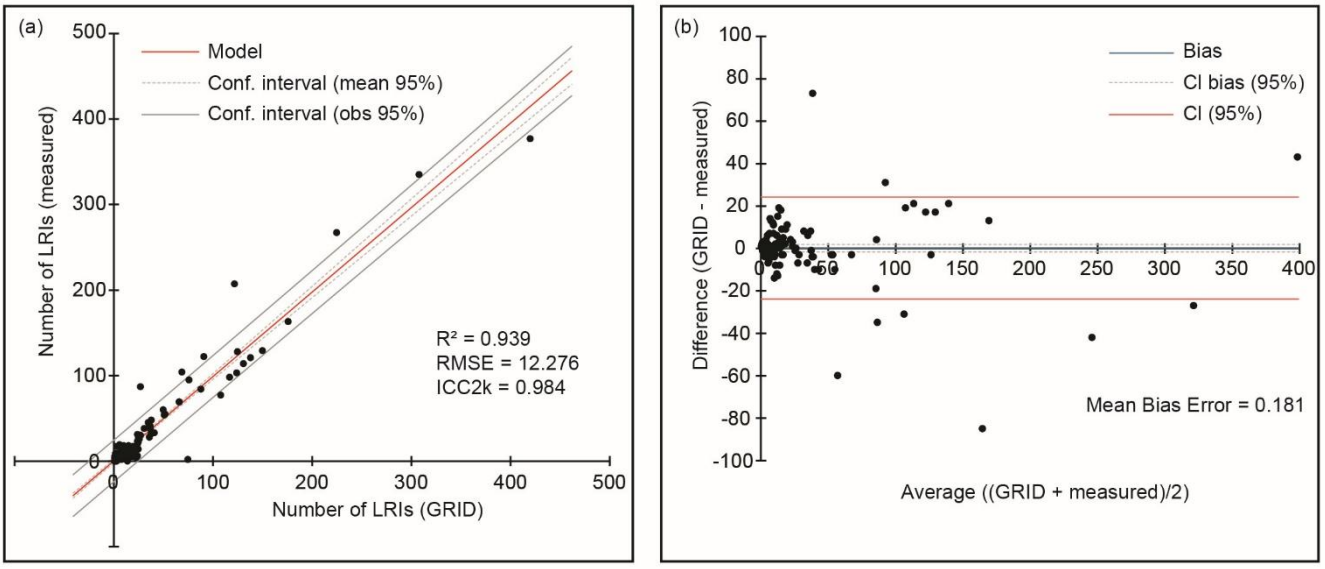

Figure 6: Relationship between the number of LRIs estimated within the GRID and those measured from satellite imagery. (a) linear regression plot and (b) Bland-Altman plot of mean bias error.

4.3 Comparison to other shoreline datasets

The initial LRI filtering methods applied to GRID (size < 30km^2, elevation < 16 m, located within 1 km of coral reef) were applied to five available open access, spatially explicit shoreline datasets (Table 4). A number of interpretations can be drawn from the assessment.

Firstly, GRID is comparable to both the GSV (Sayre et al., 2019) and recently downloaded OSM data (https://osmdata.openstreetmap.de/data/land-polygons.html) with respect to the number of LRIs identified and their total land coverage. In comparison, the GSHHS (Wessel and Smith, 1996), a widely used shoreline vector dataset, contains about 64% of the total LRIs identified in GRID and appears to underestimate the number of smaller LRIs (< 1 km^2) while overestimating the number of larger islands (> 1 km^2) (Table 4). A more detailed examination discovers a tendency in the GSHHS to overestimate the size of many islands due to a coarser vector resolution in comparison to the GSV, GRID, and OSM data. The GADM database (https://gadm.org/), also commonly used in global island studies, contains less than a third of the LRIs identified in GRID. Although LRIs greater than 1 km^2 are similar in number (Table 4), many smaller islands are completely missing from the GADM (Fig. 7). The global shoreline vector file available from Natural Earth Data (https://www.naturalearthdata.com/) is the least detailed of the available datasets and only suitable for relatively coarse analyses in comparison to the others (Table 4). For example, only 1,189 LRIs are identified globally, which is less than the number of LRIs occurring throughout the Maldives alone (Khan et al., 2002).

https://doi.org/10.5194/essd-2025-833
Preprint. Discussion started: 15 January 2026

Table 4. Global occurrences of LRIs derived from publicly available shoreline datasets.

		LRIs ≤ 1 km^2	LRIs >1 km^2	Total
Islands (n)	GADM	8,338	1,721	10,059
	GRID	32,483	1,921	34,404
	GSHHS	19,331	2,607	21,938
	GSV	26,356	1,849	28,205
	Natural Earth	608	581	1,189
	OSM	34,682	1,682	36,364
Area (km^2)	GADM	1,522	7,452	8,974
	GRID	2,355	8,544	10,899
	GSHHS	3,624	10,776	14,399
	GSV	2,349	8,289	10,638
	Natural Earth	134	4,762	4,897
	OSM	2,329	7,200	9,529
Length of shoreline (km)	GADM	15,666	23,567	39,233
	GRID	32,092	28,651	60,742
	GSHHS	31,695	29,455	61,149
	GSV	29,158	25,848	55,006
	Natural Earth	1,248	8,673	9,922
	OSM	34,245	24,486	58,731

Secondly, a visual comparison of the datasets reveals the coarse nature of the Natural Earth dataset that is noticeable even at map scales of ~ 1: 130,000 (Fig. 8). The GSHHS and GADM perform moderately in terms of capturing the numbers of LRIs but it is clear from the analysis that the GSHHS and the Natural Earth dataset have inconsistent georeferencing and can be misaligned by as much as 3 km. GRID, GSV and OSM data are most accurate with respect to geospatial alignment (Fig. 8). However, it is important to note that LRIs within the GRID can, on rare occasions, also be misaligned, which can be attributed to errors in the original GID2.1 shoreline vector file that is based on older OSM data. It is anticipated that future versions of GRID could utilise current OSM data to improve estimates.

At finer map scales (e.g., 1:5000), it becomes apparent that OSM and GRID outperform other shoreline datasets on many Pacific atolls, where numerous LRIs are separated by shallow passages of reef flat (hoa). The more recent GSV was developed using 30 m resolution Landsat satellite imagery and a semi-automated classification of land and water, and is one of the more accurate shoreline datasets tested. However, the classification algorithm implemented for the GSV has failed to identify these

https://doi.org/10.5194/essd-2025-833
Preprint. Discussion started: 15 January 2026

shallow water hoa on a number of occasions and has thus led to the merging of LRIs (see Fig. S4). It is important to note that this problem is not restricted to the GSV and can occur with any of the shoreline datasets indicating improvements are required.

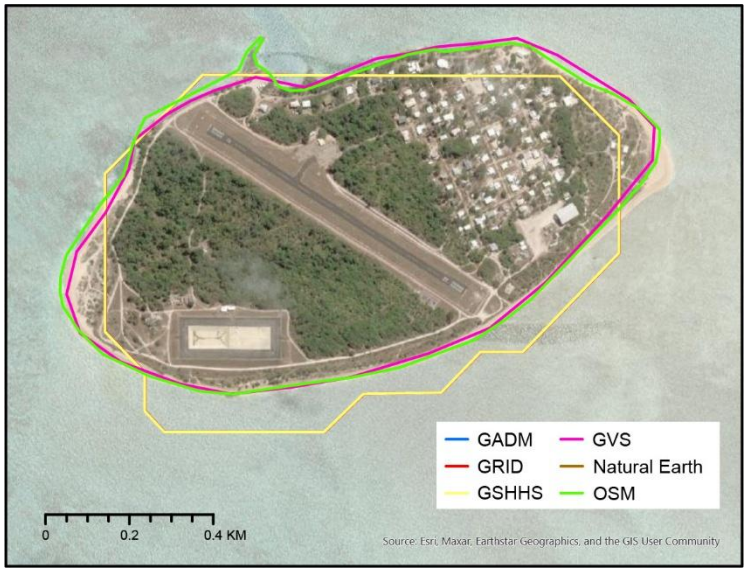

395 **Figure 7: A georeferenced satellite image of a small LRI (Warraber, The Torres Strait) overlain by six shoreline datasets. Note that the GADM and Natural Earth datasets are absent.**

5 Proposed CVI approach to LRIs

Having developed the GRID as a foundation for developing LRI-specific CVIs, the anticipated next step would be to decide
400 upon the variables with which to build the vulnerability index. Variables should represent significant driving processes influencing the island vulnerability. In this example, the variables are selected based on scientific knowledge and include mean elevation, area, length of coastline, circularity, tidal range, mean annual wave height, wave energy exposure, tropical storm exposure, sea-level rise, and population (see Table S2).

Following variable selection, a normalisation procedure is required to place them on a single, unitless scale that allows direct
405 comparison. It is also recommended to transform data, prior to normalisation, where required. In this example, each variable is cube root-transformed and a min-max normalisation technique applied using Eq. 1 when a variable has positive influence and Eq. 2 when a variable has negative influence:

$$\bar{X}_{ij} = \frac{X_{ij} - Min_i\{X_{ij}\}}{Max_i\{X_{ij}\} - Min_i\{X_{ij}\}}, \quad (1)$$

410

https://doi.org/10.5194/essd-2025-833
Preprint. Discussion started: 15 January 2026

Open Access Earth System Science Data Discussions

$$\bar{X}_{ij} = \frac{Max_i\{X_{ij}\} - X_{ij}}{Max_i\{X_{ij}\} - Min_i\{X_{ij}\}}, \quad (2)$$

where X is the original value and $\bar{X}$ is the normalised value for LRI i and variable j.

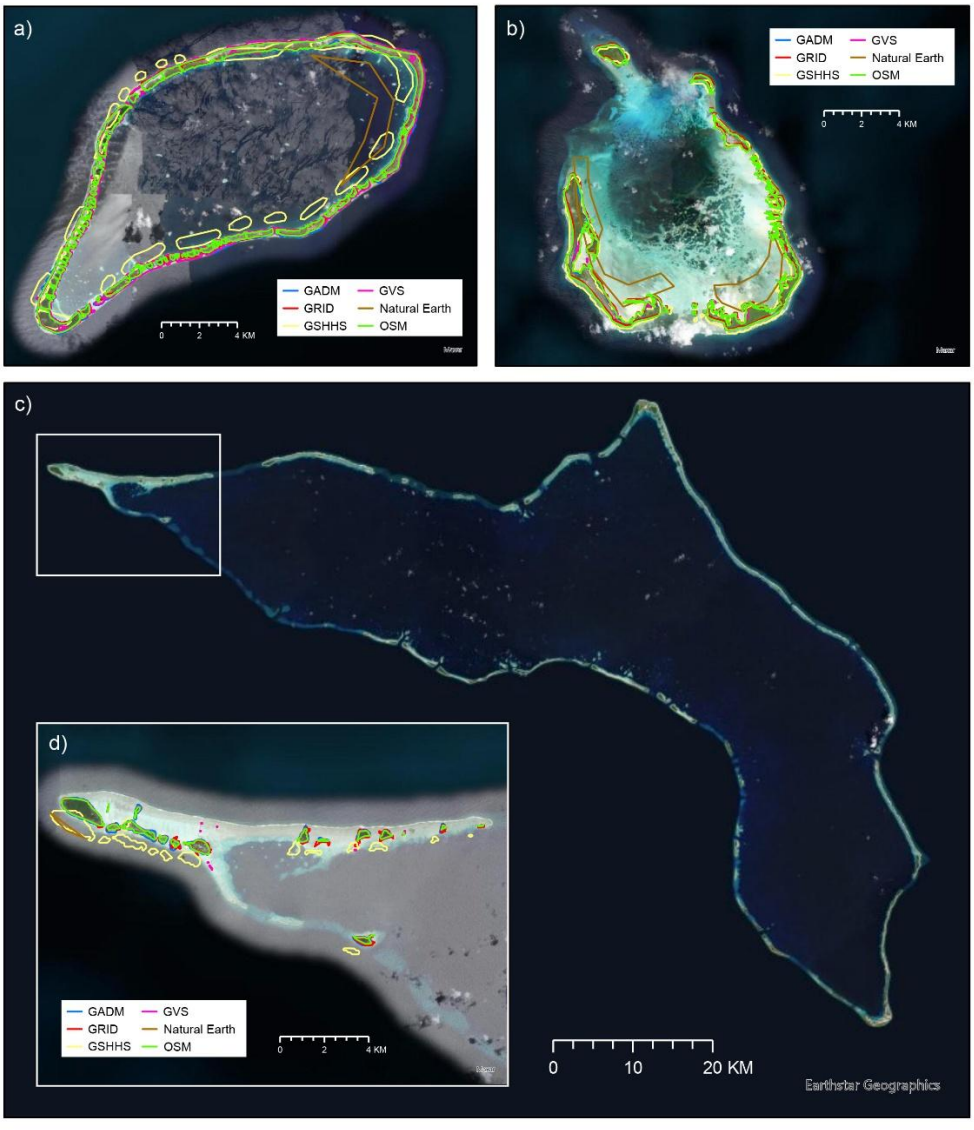

415

Figure 8: A visual assessment of existing global shoreline datasets. (a) Ahe Atoll, Tuamotus, (b) Cocos Keeling Islands and (c-d) Kwajalein Atoll, Republic of the Marshall Islands.

https://doi.org/10.5194/essd-2025-833
Preprint. Discussion started: 15 January 2026

Open Access Earth System Science Data Discussions

A critical next step is to decide on the weighting of the normalised variables. There are various methods of weighting variables including equal weighting (Kumar et al., 2018; Koroglu et al., 2019; Ahmed et al., 2022), expert judgement (Halpern et al., 2008), inverse variance method (Iyengar and Sudarshan, 1982), or multivariate statistical techniques (Ablain et al., 2017; Tanir et al., 2021; Bucherie et al., 2022). For this example, a Principal Component Analysis (PCA) is used to assign appropriate weights using Eq. 3:

$$W_j = \sum_{k=1}^{n} |L_{jk}| E_k, \quad (3)$$

where W_j is the weight of variable j, n is the number of k factors retained in the PCA, L_{jk} is the loading of variable j for principal component factor k, and E_k is the eigenvalue of factor k. Four principal components were retained in this example based on an eigenvalue above or close to 1 (Bucherie et al., 2022).

The next step is to integrate the weighted variables into a single island vulnerability index (IVI) for each LRI using Eq. 4:

$$IVI_i = \frac{\sum \bar{x}_{ij} w_{ij}}{\sum w_{ij}}, \quad (4)$$

where IVI_i is the vulnerability index of LRI i. Final IVI will fall on a scale of between 0-1 with 0 representing no vulnerability and 1 representing maximum vulnerability. Optionally, the vulnerability indices can be normalised again so that 0 and 1 represents the minimum and maximum vulnerability scores exhibited by LRIs in the GRID. Both IVI_i and normalised IVI_i are included in the GRID under the headings *IVI* and *IVINorm*.

Fig. 9 provides an example of how the GRID can provide a spatial foundation for a globally consistent indicative index of relative vulnerability of LRIs to climate change. Over two-thirds (23,777) of all LRIs are classified into either low (22%), moderate (22%) or high (26%) vulnerability classes, whilst 15% (5,120) are classified as having very low vulnerability and 16% (5,506) are classified as having very high vulnerability. Most of the LRIs with the highest vulnerability occur in the northwest Pacific including the northern Philippines, northern parts of the South China Sea and the Ryukyu Islands that extend from Taiwan to Japan (Fig.9). These areas are consistent with the regions of highest tropical storm exposure and, to a lesser extent, the fastest rates of projected sea-level rise (Fig. 5). Conversely, the majority of LRIs with the lowest vulnerability occur throughout Indonesia, the Red Sea and the Persian Gulf.

The GRID provides an opportunity to assess the vulnerability of LRIs at a national scale. The distribution and median values of the normalised IVI for 118 countries and territories are shown in Fig. 10. The results show that six countries/territories (China, the South China Sea conflict zone, Japan, Northern Mariana Islands, Paracel Islands, and Taiwan) have at least half of their LRIs classified as very highly vulnerable. Conversely, fourteen countries/territories have at least half of their LRIs classified as having very low vulnerability and include Bahrain, Egypt, Eritrea, Howland Island and Baker Island, Indonesia, Iran, Jarvis Island, Kuwait, Papua New Guinea, Qatar, Saudi Arabia, Sudan, Sudan/Egypt contested, and Yemen. There is

https://doi.org/10.5194/essd-2025-833
Preprint. Discussion started: 15 January 2026

large variation in vulnerability at a national scale (within countries) (Fig. 10). For example, only twelve countries/territories fall entirely within a single vulnerability class and only two of those contain more than one LRI (Bassas da India and Wake Island). The largest spread of LRI vulnerabilities occurs in the Philippines and Australia, indicated by their respective 5th and 95th percentiles (Fig. 10). Within the Philippines, normalised IVI almost covers the entire vulnerability scale (0.080-0.958), whereas normalised IVI in Australia ranges from 0.113 to 0.875. Of the top 20 countries/territories by number of LRIs (see Fig. 3) only Japan has a median normalised IVI of >0.699 (very high vulnerability). However, of particular concern is that 12 of the top 20 countries/territories have a median normalised IVI of >0.555 (high to very high vulnerability) (Fig. S5). Furthermore, most vulnerable LRIs (IVI >0.699) provide land for almost half a million people worldwide, many of which may be forced to migrate elsewhere in response to climate change impacts such as sea-level rise (Remling, 2020).

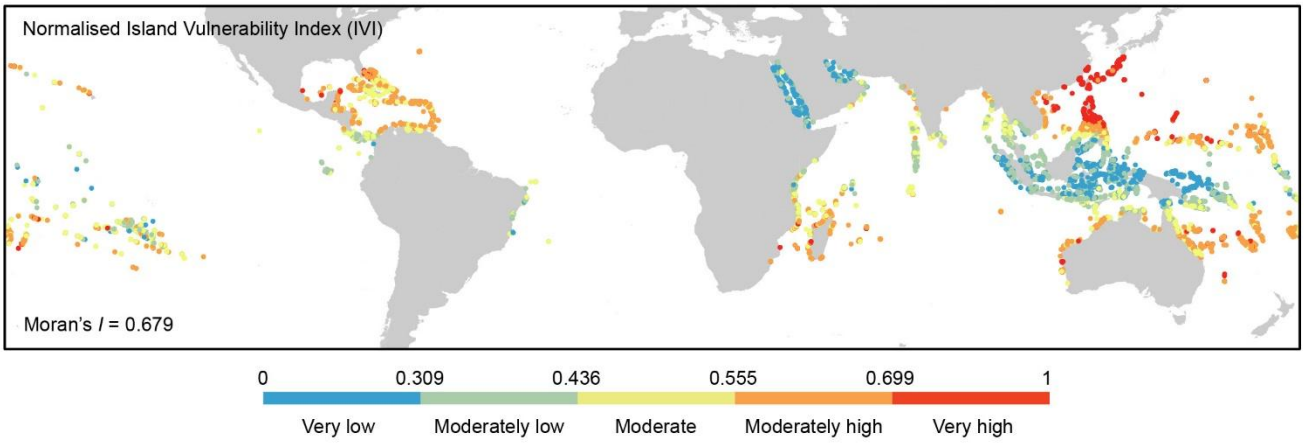

Figure 9: Global index of relative vulnerability of LRIs to climate change based on data contained within the GRID.

6 Data availability

The GRID database is provided as ESRI shapefiles (points and polygons in WGS84 and Mollweide projection), a tab-delimited text file and a comma-separated value file. All associated datasets can be downloaded from the PANGAEA data repository at https://doi.org/10.1594/PANGAEA.986811 (Dawson, 2025).

7 Conclusions

This work presents the first globally consistent, spatially comprehensive database of low-lying reef islands (LRIs), filling a major gap in coastal and climate-vulnerability research. The Global Reef Island Database (GRID), integrated from multiple sources, identified more than 34,404 LRIs, far exceeding previous global estimates and providing the most detailed

https://doi.org/10.5194/essd-2025-833
Preprint. Discussion started: 15 January 2026

quantification to date. LRIs are heavily concentrated in Asia and Oceania and the vast majority (94%) are <1 km^2 in size, demonstrating high risk and geomorphological sensitivity.

The dataset captures expected high spatial variability in certain extrinsic variables such as wave exposure, tides, storm frequency and projected sea-level rise, creating distinct regional "risk hotspots". The northwest Pacific, northern Philippines, South China Sea and Ryukyu Islands emerge as areas with the highest overall vulnerability, driven largely by high storm exposure and rapid projected sea-level rise. Conversely, LRIs in Indonesia, the Red Sea and the Persian Gulf show generally lower vulnerability scores.

Using GRID, a new globally consistent Island Vulnerability Index (IVI) was developed for LRIs with two-thirds of islands falling into low, moderate, or high vulnerability classes, and 16% classified as very highly vulnerable. Several countries including China and the disputed islands of the South China Sea, Japan, Northern Mariana Islands, Paracel Islands and Taiwan have a majority of their LRIs in the highest risk category, implying significant implications for national adaptation planning. Furthermore, the most vulnerable LRIs collectively host nearly half a million people, highlighting human exposure to climate-driven hazards like sea-level rise and storm impacts.

Validation using both published studies and satellite observations shows high accuracy and strong agreement, confirming the reliability of GRID. However, uncertainties remain due to variation in source datasets, DEM inaccuracies and the inherently dynamic nature of reef islands. Future improvements could incorporate newer satellite datasets, improved machine learning approaches, and more precise elevation models. Nevertheless, GRID provides a crucial foundation for future global, regional and local assessments of climate risk, adaptation planning and conservation prioritisation, enabling more accurate and equitable vulnerability assessments for small island nations, which have often been underrepresented or misrepresented in previous global datasets.

https://doi.org/10.5194/essd-2025-833
Preprint. Discussion started: 15 January 2026

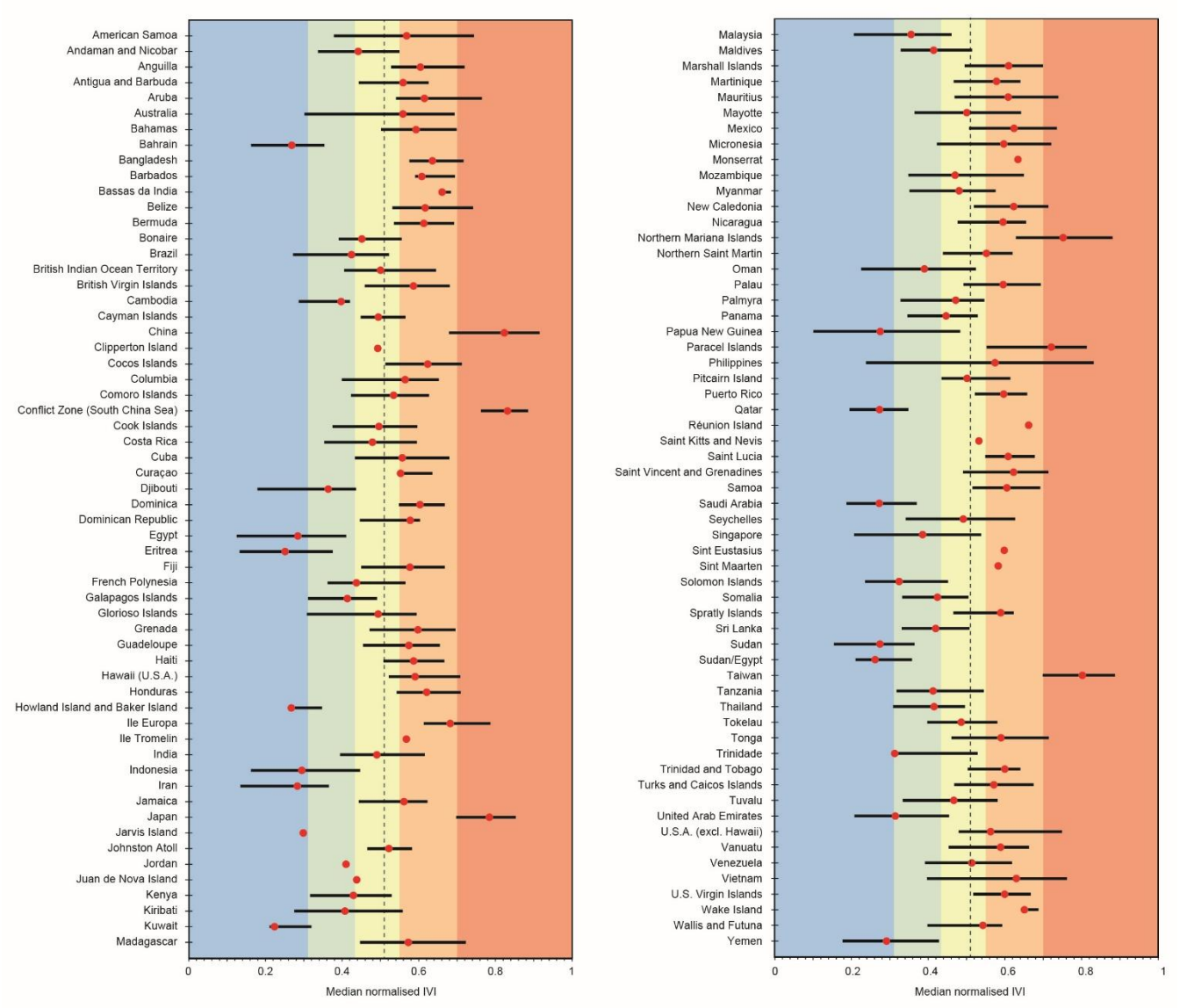

Figure 10: Relative vulnerability of LRIs to climate change at national scale. Dots and horizontal lines represent the median and range of normalised island vulnerability index (IVI) for LRIs in each country, respectively. Colour gradations from blue to red represent the five scales of island vulnerability (very low, moderately low, moderate, moderately high and very high).

Competing interests.

The author declares that they have no conflict of interest.

https://doi.org/10.5194/essd-2025-833
Preprint. Discussion started: 15 January 2026

References

Ablain, M., Legeais, J. F., Prandi, P., Marcos, M., Fenoglio-Marc, L., Dieng, H. B., Benveniste, J., and Cazenave, A.: Satellite Altimetry-Based Sea Level at Global and Regional Scales, Surv. Geophys., 38, 7-31, https://doi.org/10.1007/s10712-016-9389-8, 2017.

Ahmed, M. A., Sridharan, B., Saha, N., Sannasiraj, S. A., and Kuiry, S. N.: Assessment of coastal vulnerability for extreme events, IJDRR, 82, 103341, https://doi.org/10.1016/j.ijdrr.2022.103341, 2022.

Albert, S., Leon, J. X., Grinham, A. R., Church, J. A., Gibbes, B. R., and Woodroffe, C. D.: Interactions between sea-level rise and wave exposure on reef island dynamics in the Solomon Islands, Environ. Res. Lett., 11, 054011, https://doi.org/10.1088/1748-9326/11/5/054011, 2016.

Bai, Z., Wang, J., Wang, M., Gao, M., and Sun, J.: Accuracy Assessment of Multi-Source Gridded Population Distribution Datasets in China, Sustainability, 10, 1363, https://doi.org/10.3390/su10051363, 2018.

Baker, N., Beger, M., McClennen, C., Ishoda, A., and Edwards, F.: Reimaanlok: A National Framework for Conservation Area Planning in the Marshall Islands, J. Mar. Biol., 2011, 11, https://doi.org/10.1155/2011/273034, 2011.

Becker, M., Meyssignac, B., Letetrel, C., Llovel, W., Cazenave, A., and Delcroix, T.: Sea level variations at tropical Pacific islands since 1950, Global Planet. Change, 80–81, 85-98, https://doi.org/10.1016/j.gloplacha.2011.09.004, 2012.

Beetham, E., Kench, P. S., and Popinet, S.: Future Reef Growth Can Mitigate Physical Impacts of Sea-Level Rise on Atoll Islands, Earth's Future, 5, 1002-1014, https://doi.org/10.1002/2017EF000589, 2017.

Bentley, S. J. and Nittrouer, C. A.: Accumulation and intense bioturbation of bioclastic muds along a carbonate-platform margin: Dry Tortugas, Florida, Mar. Geol., 315-318, 44-57, https://doi.org/10.1016/j.margeo.2012.05.002, 2012.

Bland, J. M. and Altman, D. G.: A note on the use of the intraclass correlation coefficient in the evaluation of agreement between two methods of measurement, Comput. Biol. Med., 20, 337-340, https://doi.org/10.1016/0010-4825(90)90013-F, 1990.

Bucherie, A., Hultquist, C., Adamo, S., Neely, C., Ayala, F., Bazo, J., and Kruczkiewicz, A.: A comparison of social vulnerability indices specific to flooding in Ecuador: principal component analysis (PCA) and expert knowledge, IJDRR, 73, 102897, https://doi.org/10.1016/j.ijdrr.2022.102897, 2022.

Caglar, B., Becek, K., Mekik, C., and Ozendi, M.: On the vertical accuracy of the ALOS world 3D-30m digital elevation model, Remote Sens. Lett., 9, 607-615, https://doi.org/10.1080/2150704X.2018.1453174, 2018.

Chand, S. S.: Climate Change Scenarios and Projections for the Pacific, in: Climate Change and Impacts in the Pacific, edited by: Kumar, L., Springer International Publishing, Cham, 171-199, https://doi.org/10.1007/978-3-030-32878-8_3, 2020.

Dawson, J. L.: A spatially explicit Global Reef Island Database (GRID) that captures distribution, diversity and relative vulnerability of the world's low-lying reef islands [dataset]. PANGAEA, https://doi.org/10.1594/PANGAEA.986811, 2025.

DeCarlo, T. M., Cohen, A. L., Barkley, H. C., Cobban, Q., Young, C., Shamberger, K. E., Brainard, R. E., and Golbuu, Y.: Coral macrobioerosion is accelerated by ocean acidification and nutrients, Geology, 43, 7-10, https://doi.org/10.1130/g36147.1, 2015.

Dunne, R. P., Barbosa, S. M., and Woodworth, P. L.: Contemporary sea level in the Chagos Archipelago, central Indian Ocean, Global Planet. Change, 82-83, 25-37, https://doi.org/10.1016/j.gloplacha.2011.11.009, 2012.

Duvat, V., Volto, N., and Salmon, C.: Impacts of category 5 tropical cyclone Fantala (April 2016) on Farquhar Atoll, Seychelles Islands, Indian Ocean, Geomorphology, 298, https://doi.org/10.1016/j.geomorph.2017.09.022, 2017a.

Duvat, V. K. E., Salvat, B., and Salmon, C.: Drivers of shoreline change in atoll reef islands of the Tuamotu Archipelago, French Polynesia, Global Planet. Change, 158, 134-154, https://doi.org/10.1016/j.gloplacha.2017.09.016, 2017b.

Dvorak, G.: Coral and Concrete: Remembering Kwajalein Atoll between Japan, America, and the Marshall Islands, University of Hawai'i Press, 346 pp.2018.

East, H. K., Perry, C. T., Kench, P. S., Liang, Y., and Gulliver, P.: Coral Reef Island Initiation and Development Under Higher Than Present Sea Levels, Geophys. Res. Lett., 45, 11,265-211,274, https://doi.org/10.1029/2018gl079589, 2018.

Evans, S. N., Konzewitsch, N., and Bellchambers, L. M.: Houtman Abrolhos Islands Fish Habitat Protection Area: A Summary of Marine Resource Use and Ecological Attributes, in: Fisheries Research Report No. 321, Department of Primary Industries and Regional Development, Western Australia, 1-174, 2022.

https://doi.org/10.5194/essd-2025-833
Preprint. Discussion started: 15 January 2026

Falkland, T. and White, I.: Freshwater Availability Under Climate Change, in: Climate Change and Impacts in the Pacific, edited by: Kumar, L., Springer International Publishing, Cham, 403-448, https://doi.org/10.1007/978-3-030-32878-8_11, 2020.
Ferrario, F., Beck, M. W., Storlazzi, C. D., Micheli, F., Shepard, C. C., and Airoldi, L.: The effectiveness of coral reefs for coastal hazard risk reduction and adaptation, Nat. Commun., 5, 3794, https://doi.org/10.1038/ncomms4794, 2014.
Ford, M.: Shoreline changes interpreted from multi-temporal aerial photographs and high resolution satellite images: Wotje Atoll, Marshall Islands, Remote Sens. Environ., 135, 130-140, https://doi.org/10.1016/j.rse.2013.03.027, 2013.
Gillespie, R. G. and Clague, D. A.: Encyclopedia of Islands, 1, University of California Press2009.
Gornitz, V. and Kanciruk, P.: Assessment of global coastal hazards from sea level rise, Coastal Zone '89: Proceedings of the Sixth Symposium on Coastal and Ocean Management, Charleston, SC, USA1989.
Gornitz, V. M., Daniels, R. C., White, T. W., and Birdwell, K. R.: The development of a coastal risk assessment database: vulnerability to sea-level rise in the US Southeast, J. Coast. Res., 327-338, 1994.
Halpern, B. S., Walbridge, S., Selkoe, K. A., Kappel, C. V., Micheli, F., D'Agrosa, C., Bruno, J. F., Casey, K. S., Ebert, C., Fox, H. E., Fujita, R., Heinemann, D., Lenihan, H. S., Madin, E. M. P., Perry, M. T., Selig, E. R., Spalding, M., Steneck, R., and Watson, R.: A Global Map of Human Impact on Marine Ecosystems, Science, 319, 948-952, https://doi.org/10.1126/science.1149345, 2008.
Harris, D. L., Rovere, A., Casella, E., Power, H., Canavesio, R., Collin, A., Pomeroy, A., Webster, J. M., and Parravicini, V.: Coral reef structural complexity provides important coastal protection from waves under rising sea levels, Sci. Adv., 4, eaao4350, https://doi.org/10.1126/sciadv.aao4350, 2018.
Hilton, M. J., Borrie, D. R., Konlechner, T. M., Wakes, S. J., Lane, T. P., Kench, P. S., Kennedy, D. M., and Aslam, M.: A first evaluation of the contribution of aeolian sand transport to lagoon island accretion in the Maldives, Aeolian Res., 39, 47-65, https://doi.org/10.1016/j.aeolia.2019.04.006, 2019.
Hoeke, R. K., Damlamian, H., Aucan, J., and Wandres, M.: Severe Flooding in the Atoll Nations of Tuvalu and Kiribati Triggered by a Distant Tropical Cyclone Pam, Front. Mar. Sci., 7, https://doi.org/10.3389/fmars.2020.539646, 2021.
Hopley, D., Smithers, S. G., and Parnell, K.: Islands of the Great Barrier Reef, in: The Geomorphology of the Great Barrier Reef: Development, Diversity and Change, edited by: Hopley, D., Smithers, S. G., and Parnell, K., Cambridge University Press, Cambridge, 311-366, https://doi.org/10.1017/CBO9780511535543.011, 2007.
Hughes, T. P., Barnes, M. L., Bellwood, D. R., Cinner, J. E., Cumming, G. S., Jackson, J. B. C., Kleypas, J., van de Leemput, I. A., Lough, J. M., Morrison, T. H., Palumbi, S. R., van Nes, E. H., and Scheffer, M.: Coral reefs in the Anthropocene, Nature, 546, 82-90, https://doi.org/10.1038/nature22901, 2017.
Iese, V., Halavatau, S., N'Yeurt, A. D. R., Wairiu, M., Holland, E., Dean, A., Veisa, F., Patolo, S., Havea, R., Bosenaqali, S., and Navunicagi, O.: Agriculture Under a Changing Climate, in: Climate Change and Impacts in the Pacific, edited by: Kumar, L., Springer International Publishing, Cham, 323-357, https://doi.org/10.1007/978-3-030-32878-8_9, 2020.
Iyengar, N. S. and Sudarshan, P.: A Method of Classifying Regions from Multivariate Data, Econ. Polit. Wkly, 17, 2047-2052, 1982.
Karnauskas, K. B., Donnelly, J. P., and Anchukaitis, K. J.: Future freshwater stress for island populations, Nat. Clim. Chang., 6, 720-725, https://doi.org/10.1038/nclimate2987, 2016.
Kayanne, H., Yasukochi, T., Yamaguchi, T., Yamano, H., and Yoneda, M.: Rapid settlement of Majuro Atoll, central Pacific, following its emergence at 2000 years CalBP, Geophys. Res. Lett., 38, https://doi.org/10.1029/2011GL049163, 2011.
Kench, P.: The geomorphology of Baa (South Maalhosmadulu) Atoll and its reef islands, Atoll Res. Bull., 1-29, https://doi.org/10.1007/s003380050110, 2012.
Kench, P., Perry, C., and Spencer, T.: Coral reefs, in: Geomorphology and Global Environmental Change, edited by: Embleton-Hamann, C., Slaymaker, O., and Spencer, T., Cambridge University Press, Cambridge, 180-213, https://doi.org/10.1017/CBO9780511627057.008, 2009.
Kench, P. S. and Brander, R. W.: Response of reef island shorelines to seasonal climate oscillations: South Maalhosmadulu atoll, Maldives, J. Geophys. Res. Earth Surf., 111, https://doi.org/10.1029/2005JF000323, 2006.
Kench, P. S., Owen, S. D., and Ford, M. R.: Evidence for coral island formation during rising sea level in the central Pacific Ocean, Geophys. Res. Lett., 41, 820-827, https://doi.org/10.1002/2013GL059000, 2014.

https://doi.org/10.5194/essd-2025-833
Preprint. Discussion started: 15 January 2026

Khan, T. M. A., Quadir, D. A., Murty, T. S., Kabir, A., Aktar, F., and Sarker, M. A.: Relative Sea Level Changes in Maldives and Vulnerability of Land Due to Abnormal Coastal Inundation, Mar. Geod., 25, 133-143, https://doi.org/10.1080/014904102753516787, 2002.

Kirtman, B., Power, S. B., Adedoyin, J. A., Boer, G. J., Bojariu, R., Camilloni, I., Doblas-Reyes, F. J., Fiore, A. M., Kimoto, M., Meehl, G. A., Prather, M., Sarr, A., Schär, C., Sutton, R., van Oldenborgh, G. J., Vecchi, G., and Wang, H. J.: Near-term Climate Change: Projections and Predictability, in: Climate Change 2013: The Physical Science Basis. Contribution of Working Group I to the Fifth Assessment Report of the Intergovernmental Panel on Climate Change, edited by: Stocker, T. F., Qin, D., Plattner, G.-K., Tignor, M., Allen, S. K., Boschung, J., Nauels, A., Xia, Y., Bex, V., and Midgley, P. M., Cambridge University Press, Cambridge, United Kingdom and New York, NY, USA, 953–1028, https://doi.org/10.1017/CBO9781107415324.023, 2013.

Koo, T. K. and Li, M. Y.: A Guideline of Selecting and Reporting Intraclass Correlation Coefficients for Reliability Research, J Chiropr Med, 15, 155-163, https://doi.org/10.1016/j.jcm.2016.02.012, 2016.

Koroglu, A., Ranasinghe, R., Jiménez, J. A., and Dastgheib, A.: Comparison of Coastal Vulnerability Index applications for Barcelona Province, Ocean Coast. Manage., 178, 104799, https://doi.org/10.1016/j.ocecoaman.2019.05.001, 2019.

Kumar, L. and Tehrany, M. S.: Climate change impacts on the threatened terrestrial vertebrates of the Pacific Islands, Sci Rep., 7, 5030, https://doi.org/10.1038/s41598-017-05034-4, 2017.

Kumar, L., Jayasinghe, S., Gopalakrishnan, T., and Nunn, P. D.: Climate Change and the Pacific Islands, in: Climate Change and Impacts in the Pacific, edited by: Kumar, L., Springer International Publishing, Cham, 1-31, https://doi.org/10.1007/978-3-030-32878-8_1, 2020.

Kumar, L., Eliot, I., Nunn, P. D., Stul, T., and McLean, R.: An indicative index of physical susceptibility of small islands to coastal erosion induced by climate change: an application to the Pacific islands, Geomat. Nat. Hazards Risk, 9, 691-702, https://doi.org/10.1080/19475705.2018.1455749, 2018.

Lavers, J. L., Dicks, L., Dicks, M. R., and Finger, A.: Significant plastic accumulation on the Cocos (Keeling) Islands, Australia, Sci Rep., 9, 7102, https://doi.org/10.1038/s41598-019-43375-4, 2019.

Maragos, J. E., Graham, B. K. B., and Beveridge, P. J.: Tropical Cyclone Bebe Creates a New Land Formation on Funafuti Atoll, Science, 181, 1161-1164, https://doi.org/10.1126/science.181.4105.1161, 1973.

McLean, R.: Atoll Islands (Motu), in: Encyclopedia of Modern Coral Reefs, edited by: Hopley, D., Springer Dordrecht, 47-51, 2011.

Meinshausen, M., Nicholls, Z. R. J., Lewis, J., Gidden, M. J., Vogel, E., Freund, M., Beyerle, U., Gessner, C., Nauels, A., Bauer, N., Canadell, J. G., Daniel, J. S., John, A., Krummel, P. B., Luderer, G., Meinshausen, N., Montzka, S. A., Rayner, P. J., Reimann, S., Smith, S. J., van den Berg, M., Velders, G. J. M., Vollmer, M. K., and Wang, R. H. J.: The shared socio-economic pathway (SSP) greenhouse gas concentrations and their extensions to 2500, Geosci. Model Dev., 13, 3571-3605, https://doi.org/10.5194/gmd-13-3571-2020, 2020.

Murray, M. R., Zisman, S., and Minty, C. D.: Soil-Plant Relationships and A Revised Vegetation Classification of Turneffe Atoll, Belize, Atoll Res. Bull., 4, 1-32, https://doi.org/10.1016/j.jenvman.2009.06.018, 1999.

Nicholls, R. J. and Cazenave, A.: Sea-Level Rise and Its Impact on Coastal Zones, Science, 328, 1517-1520, https://doi.org/10.1126/science.1185782, 2010.

Nunn, P. D. and Britton, J. M. R.: Human-Environment Relationships in the Pacific Islands around A.D. 1300, Environ. Hist., 7, 3-22, https://doi.org/10.3197/096734001129342388, 2001.

Nunn, P. D., Kumar, L., Eliot, I., and McLean, R. F.: Classifying Pacific islands, Geosci. Lett., 3, 7, https://doi.org/10.1186/s40562-016-0041-8, 2016.

Nunn, P. D., Kumar, L., McLean, R., and Eliot, I.: Islands in the Pacific: Settings, Distribution and Classification, in: Climate Change and Impacts in the Pacific, edited by: Kumar, L., Springer International Publishing, Cham, 33-170, https://doi.org/10.1007/978-3-030-32878-8_2, 2020.

Nurse, L. A., McLean, R. F., Agard, J., Briguglio, L. P., Duvat-Magnan, V., Pelesikoti, N., Tompkins, E., and Webb, A.: Small islands, in: Climate Change 2014: Impacts, Adaptation, and Vulnerability. Part B: Regional Aspects. Contribution of Working Group II to the Fifth Assessment Report of the Intergovernmental Panel of Climate Change, edited by: Barros, V. R., Field, C. B., Dokken, D. J., Mastrandrea, M. D., Mach, K. J., Bilir, T. E., Chatterjee, M., Ebi, K. L., Estrada, Y. O., Genova, R. C., Girma, B., Kissel, E. S., Levy, A. N., MacCracken, S., Mastrandrea, P. R., and White, L. L., Cambridge University Press, Cambridge, United Kingdom and New York, NY, USA, 1613-1654, 2014.

https://doi.org/10.5194/essd-2025-833
Preprint. Discussion started: 15 January 2026

Osawa, Y., Fujita, K., Umezawa, Y., Kayanne, H., Ide, Y., Nagaoka, T., Miyajima, T., and Yamano, H.: Human impacts on large benthic foraminifers near a densely populated area of Majuro Atoll, Marshall Islands, Mar. Pollut. Bull., 60, 1279-1287, https://doi.org/10.1016/j.marpolbul.2010.03.014, 2010.

Paris, P. and Mitasova, H.: Barrier Island Dynamics Using Mass Center Analysis: A New Way to Detect and Track Large-Scale Change, ISPRS Int. J. Geo-Inf., 3, 49-65, https://doi.org/10.3390/ijgi3010049, 2014.

Perry, C. T., Kench, P. S., Smithers, S. G., Riegl, B., Yamano, H., and O'Leary, M. J.: Implications of reef ecosystem change for the stability and maintenance of coral reef islands, Global Change Biol., 17, 3679-3696, https://doi.org/10.1111/j.1365-2486.2011.02523.x, 2011.

Remling, E.: Migration as climate adaptation? Exploring discourses amongst development actors in the Pacific Island region, Reg. Environ. Change, 20, 3, https://doi.org/10.1007/s10113-020-01583-z, 2020.

Santillan, J. R., Makinano-Santillan, M., and Makinano, R. M.: Vertical accuracy assessment of ALOS World 3D - 30M Digital Elevation Model over northeastern Mindanao, Philippines, 2016 IEEE International Geoscience and Remote Sensing Symposium (IGARSS), 10-15 July 2016, 5374-5377, https://doi.org/10.1109/IGARSS.2016.7730400,

Sayre, R., Noble, S., Hamann, S., Smith, R., Wright, D., Breyer, S., Butler, K., Van Graafeiland, K., Frye, C., Karagulle, D., Hopkins, D., Stephens, D., Kelly, K., Basher, Z., Burton, D., Cress, J., Atkins, K., Van Sistine, D. P., Friesen, B., Allee, R., Allen, T., Aniello, P., Asaad, I., Costello, M. J., Goodin, K., Harris, P., Kavanaugh, M., Lillis, H., Manca, E., Muller-Karger, F., Nyberg, B., Parsons, R., Saarinen, J., Steiner, J., and Reed, A.: A new 30 meter resolution global shoreline vector and associated global islands database for the development of standardized ecological coastal units, J. Oper. Oceanogr., 12, S47-S56, https://doi.org/10.1080/1755876X.2018.1529714, 2019.

Sengupta, M., Ford, M. R., Kench, P. S., and Perry, G. L. W.: Exploring the drivers of reef island shoreline change using machine learning models, Sci Rep., 15, 16735, 10.1038/s41598-025-00136-w, 2025.

Sheppard, C. R. C., Ateweberhan, M., Bowen, B. W., Carr, P., Chen, C. A., Clubbe, C., Craig, M. T., Ebinghaus, R., Eble, J., Fitzsimmons, N., Gaither, M. R., Gan, C.-H., Gollock, M., Guzman, N., Graham, N. A. J., Harris, A., Jones, R., Keshavmurthy, S., Koldewey, H., Lundin, C. G., Mortimer, J. A., Obura, D., Pfeiffer, M., Price, A. R. G., Purkis, S., Raines, P., Readman, J. W., Riegl, B., Rogers, A., Schleyer, M., Seaward, M. R. D., Sheppard, A. L. S., Tamelander, J., Turner, J. R., Visram, S., Vogler, C., Vogt, S., Wolschke, H., Yang, J. M.-C., Yang, S.-Y., and Yesson, C.: Reefs and islands of the Chagos Archipelago, Indian Ocean: why it is the world's largest no-take marine protected area, Aquat. Conserv.: Mar. Freshwat. Ecosyst., 22, 232-261, https://doi.org/10.1002/aqc.1248, 2012.

Stoddart, D. and Fosberg, F. R.: Topographic and floristic changes, dry Tortugas, Florida, 1904-1977 [Includes vegetation], Atoll Res. Bull., no. 253, 1-160, https://doi.org/10.5479/si.00775630.253.1, 1981.

Stoddart, D. R. and Steers, J. A.: 3 - The nature and origin of coral reef islands, in: Biology and Geology of Coral Reefs, edited by: Jones, O. A., and Endean, R., Academic Press, 59-105, https://doi.org/10.1016/B978-0-12-395528-9.50011-7, 1977.

Storlazzi, C. D., Gingerich, S. B., van Dongeren, A., Cheriton, O. M., Swarzenski, P. W., Quataert, E., Voss, C. I., Field, D. W., Annamalai, H., Piniak, G. A., and McCall, R.: Most atolls will be uninhabitable by the mid-21st century because of sea-level rise exacerbating wave-driven flooding, Sci. Adv., 4, https://doi.org/10.1126/sciadv.aap9741, 2018.

Summerhayes, C. P.: Lagoonal sedimentation at Aitutaki and Manuae in the Cook Islands: A reconnaissance survey, N. Z. J. Geol. Geophys., 14, 351-363, https://doi.org/10.1080/00288306.1971.10421931, 1971.

Tanir, T., Sumi, S. J., de Lima, A. d. S., de A. Coelho, G., Uzun, S., Cassalho, F., and Ferreira, C. M.: Multi-scale comparison of urban socio-economic vulnerability in the Washington, DC metropolitan region resulting from compound flooding, IJDRR, 61, 102362, https://doi.org/10.1016/j.ijdrr.2021.102362, 2021.

Thieler, E. R.: National assessment of coastal vulnerability to future sea-level rise, US Geological Survey2327-6932, 2000.

UNEP-WCMC: Global distribution of islands. Global Island Database (version 2.1, November 2015). Based on Open Street Map data (© OpenStreetMap contributors) [dataset], 2015.

Uuemaa, E., Ahi, S., Montibeller, B., Muru, M., and Kmoch, A.: Vertical Accuracy of Freely Available Global Digital Elevation Models (ASTER, AW3D30, MERIT, TanDEM-X, SRTM, and NASADEM), Remote Sens., 12, 3482, https://doi.org/10.3390/rs12213482, 2020.

Weatherdon, L. V., Fletcher, R., Jones, M. C., Kaschner, K., Sullivan, E., Tittensor, D. P., Mcowen, C., Geffert, J. L., van Bochove, J. W., Thomas, H., Blyth, S., Ravillious, C., Tolley, M., Stanwell-Smith, D., Fletcher, S., and Martin, C.: Manual of marine and coastal datasets of biodiversity importance. December 2015 edition. , Cambridge (UK): UNEP World Conservation Monitoring Centre.2015.

https://doi.org/10.5194/essd-2025-833
Preprint. Discussion started: 15 January 2026

Webb, A. P. and Kench, P. S.: The dynamic response of reef islands to sea-level rise: Evidence from multi-decadal analysis of island change in the Central Pacific, Global Planet. Change, 72, 234-246, https://doi.org/10.1016/j.gloplacha.2010.05.003, 2010.

Weigelt, P. and Kreft, H.: Quantifying island isolation – insights from global patterns of insular plant species richness, Ecography, 36, 417-429, https://doi.org/10.1111/j.1600-0587.2012.07669.x, 2013.

Weigelt, P., Jetz, W., and Kreft, H.: Bioclimatic and physical characterization of the world's islands, PNAS, 110, 15307-15312, https://doi.org/10.1073/pnas.1306309110, 2013.

Wessel, P. and Smith, W. H. F.: A global, self-consistent, hierarchical, high-resolution shoreline database, J. Geophys. Res. Solid Earth, 101, 8741-8743, https://doi.org/10.1029/96JB00104, 1996.

Woodroffe, C. D.: Reef-island topography and the vulnerability of atolls to sea-level rise, Global Planet. Change, 62, 77-96, https://doi.org/10.1016/j.gloplacha.2007.11.001, 2008.